Glycodelin acts as an immunomodulator in NSCLC and is a predictor of poor prognosis for patients receiving immunotherapy

NSCLC-derived glycodelin as an immunomodulator

Sarah Richtmann[1,2,3,4#], Sebastian Marwitz[5,6], Thomas Muley[1,2], Hannu Koistinen[7], Petros Christopoulos[2,8], Michael Thomas[2,8], Daniel Kazdal[2,9], Michael Allgäuer[9], Hauke Winter[2,10], Torsten Goldmann[5,6], Michael Meister[1,2], Ursula Klingmüller[2,3], Marc A. Schneider[1,2*]

[1]Translational Research Unit, Thoraxklinik at Heidelberg University Hospital, Heidelberg, Germany;
[2]Translational Lung Research Center Heidelberg (TLRC), Member of the German Center for Lung Research (DZL), Heidelberg, Germany;
[3]Division of Systems Biology of Signal Transduction, German Cancer Research Center (DKFZ), Heidelberg, Germany
[4]Faculty of Biosciences, University of Heidelberg, Heidelberg, Germany
[5]Histology, Research Center Borstel - Leibniz Lung Center, Borstel, Germany
[6]Airway Research Center North (ARCN), Member of the German Center for Lung Research (DZL), Borstel, Germany;
[7]Department of Clinical Chemistry and Haematology, Faculty of Medicine, University of Helsinki and Helsinki University Hospital, Finland
[8]Department of Thoracic Oncology, Thoraxklinik at Heidelberg University Hospital, Heidelberg, Germany
[9]Institute of Pathology, Heidelberg University Hospital, Heidelberg, Germany;
[10]Department of Surgery, Thoraxklinik at Heidelberg University Hospital, Heidelberg, Germany

* Corresponding author:
Marc Schneider
Thoraxklinik Heidelberg
Roentgenstrasse 1
69126 Heidelberg
marc.schneider@med.uni-heidelberg.de

Running title: Glycodelin as an immunomodulator in NSCLC

Conflicts of interest: The authors declare no conflict of interest

Abstract

Lung cancer has been shown to be targetable by novel immunotherapies which reactivate the immune system and enable tumor cell killing. However, only few patients respond to this promising approach that has the potential to cure even metastatic disease. We hypothesize that the success of the treatment is impaired by the presence of immunosuppressors in the tumor microenvironment and therefore investigated the role of the immunosuppressive glycoprotein glycodelin that is expressed in patients with non-small-cell lung cancer (NSCLC). We demonstrate that the glycan pattern of NSCLC-derived glycodelin detected by a lectin-based enrichment assay highly resembles amniotic fluid-derived glycodelin A, which is known to have immunosuppressive properties. Binding assays with different leucocyte cell lines and subsequent transcriptome analyses reveal that glycodelin indeed interacts with immune cells *in vitro* and regulates the expression of genes associated with inflammatory and tumor microenvironment pathways. Furthermore, multiplex immunofluorescence staining of glycodelin and different leucocytes in tumor microarray samples of patients with NSCLC show that glycodelin binds to tumor infiltrating CD8+ T cells and pro-tumorigenic M2 macrophages. Interestingly, we observe that high serum concentrations of glycodelin prior to immunotherapy are associated with a poor progression-free survival ($p < 0.001$) of female patients receiving PD-(L)1 inhibitors. Our findings demonstrate that glycodelin not only is a promising immunological biomarker for early identification of female patients that do not benefit from the costly immunotherapy, but also represents a promising immunotherapeutic target in NSCLC to improve therapeutic options in lung cancer.

Keywords

NSCLC, Glycodelin, Immunotherapy, Tumor microenvironment, Glycosylation

Introduction

Lung cancer is one of the most common and deadliest cancers worldwide, with an incidence of 2.2 million new cases per year and 1.8 million deaths (*1, 2*). Immunotherapies have revolutionized the landscape of cancer treatment and have enabled long-term survival in patients with metastatic non-small cell lung cancer (NSCLC) (*3*). However, not all tumors that are positive for PD-L1 show immune infiltration, and some do not respond to anti-PD-1 therapies (*4, 5*). Consequently, additional markers will be needed that cover other immune checkpoint molecules expressed on tumor cells and surrounding cells in the tumor microenvironment.

In the 1980s several investigators identified a protein, which eventually was named as glycodelin, in human placenta, in amniotic fluid, the pregnancy decidua, and seminal plasma (*6*). Glycodelin is encoded by the *progesterone-associated endometrial protein* (*PAEP*) gene and a translated from 900 bp mRNA that shares sequence similarity with bovine β-lactoglobulin (*7*) and other lipocalins (*8*). Glycodelin has been proposed to be involved in immunosuppression, angiogenesis, and apoptosis signaling during the first trimester of pregnancy [6] and to regulate fertilization and implantation (*9-11*) by immunomodulatory processes. Several differently glycosylated forms are known (*10, 12, 13*). These share the same protein backbone but highly differ in their N-glycosylation pattern. Glycodelin A is found in amniotic fluid, in the secretory and decidualized endometrium and can also be detected in the serum of women who are pre-menopausal (*9, 10, 14*). The different functions of the glycodelin-glycoforms are based on the specific glycans at Asn28 and Asn63, both located in

a conformational loop (*11*). Also, immunomodulatory effects of glycodelin have been ascribed to its glycosylation (*15*). Since pregnancy can be considered similar to a semi-allograft implantation (*16*), the maternal immune response needs to be repressed to allow a successful pregnancy. During pregnancy, Glycodelin A is the major form of glycodelin and acts as an immunomodulator on various levels. While the glycodelin has originally been found in reproductive tissues, it is also expressed in several cancers (*17, 18*). Both, *PAEP* gene expression as well as glycodelin protein expression are increased in lung adenocarcinoma (LUAD) and squamous cell carcinoma (LUSC) compared to normal lung tissues (*19, 20*). In lung cancer, *PAEP* gene expression correlated with a significantly worse overall survival in female patients (*19*).

In the past years, immunotherapy represented a major improvement in the treatment of NSCLC. Since glycodelin plays an important role in the regulation of immunosuppressive pathways and is associated with therapeutic response to immunotherapy (*21*), we characterized the interaction of glycodelin and the immune system in NSCLC.

Material and methods

Cell cultures

The cells were cultured under humidified conditions at 37 °C and 5 % CO_2. The patient-derived fibroblast cell line 4950T-F and the LUSC cell line 2427T (*22*) were cultivated in DMEM/HAMs F12 (Thermo Fisher Scientific, Waltham, Massachusetts, US) with 10 % fetal bovine serum (FBS) and 1 x stable glutamine (both Thermo Fisher Scientific). For Jurkat, THP1, and KHYG-1 (all from ATCC), RPMI 1640 (Thermo Fisher Scientific) added with 10 % FBS was used. For KHYG-1, also 10 ng/ml IL-2 (PHC0026, ThermoFisher Scientific) was added. The patient derived primary cell lines 4950T and 170162T were cultivated in serum-free DMEM/HAMs F12 with epithelial airway growth factors (C-21160, PromoCell, Heidelberg, Germany) and ROCK inhibitor (Y-27632, Merck, Darmstadt, Germany). 4950T and 170162T cell lines were characterized by immunofluorescence analyses and sequencing. Sequencing analyses revealed KRAS p.Gly13Cys for 170162T and BRAF p.Gly466Val for 4950T as main driver mutations originally detected also in the patients. A maximum amount of 20 passages was not exceeded.

Transient gene knockdown by siRNA transfection

Cells were seeded in T75 culture flasks with a cell density of 1.3 x 10^6 cells/flask and kept in the incubator at 37 °C and 5 % CO_2 overnight. For one reaction, 15 µl of siRNA (1 µM, FlexiTube GeneSolution, Qiagen, Hilden, Germany, see Table S1) were diluted in 1.5 ml culture medium without supplements. 18 µl RNAiMax (Thermo Fisher Scientific) were added and the solution was incubated for 10-20 min at room temperature. The cell culture medium was exchanged to a final volume of 13.5 ml/flask and 1.5 ml siRNA solution were carefully dripped onto the cells, resulting in a final siRNA concentration of 1 nM. Treated cells were incubated for 72 h at 37 °C and 5 % CO_2. As a control, AllStars Negative Control siRNA (Qiagen) was used.

Total RNA isolation and cDNA synthesis

For RNA isolation from cell lines, the RNeasy Mini Kit (Qiagen) was used. The complete procedure is described elsewhere (*19*). The sscDNA reaction mixtures were pooled, mixed by pipetting and separately stored in 20 µl aliquots at -20°C until further analyses.

Quantitative *Real Time* Polymerase Chain Reaction (qPCR)

Real-time quantitative PCR (qPCR) was performed in accordance with MIQE-guidelines (*23*) using a LightCycler® 480 Real-Time PCR Instrument (Roche, Mannheim, Germany) in a 384-well plate format. Gene-specific primers and probes (Universal ProbeLibrary, Roche) were used in combination with qPCR Probe-MasterMix (SL-9802, Steinbrenner, Wiesenbach, Germany). 5 ng sscDNA were usead for each amplification. The whole procedure is described elsewhere (*19*). The used primers and probes are listed in Table S2.

Patient specimens

Patient specimens were collected at Thoraxklinik-Heidelberg and stored at Lung Biobank Heidelberg. All patients signed an informed consent. The local ethics committees of the Medical Faculty Heidelberg approved the use of biomaterial and data (S-270/2001 for biobanking of specimen, S-827/2020 for the glycodelin project). The study was performed according to the principles set out in the WMA Declaration of Helsinki. Clinical parameters of the investigated patient cohorts are shown in Table 1.

Tissue sample collection, characterization and preparation

Tissue samples and tissue multi arrays (TMA) from patients with NSCLC (see table 1) were provided by the Lung Biobank Heidelberg, a member of the accredited Tissue Bank of the National Center for Tumor Diseases (NCT) Heidelberg, the BioMaterialBank Heidelberg, and the Biobank platform of the German Center for Lung Research (DZL). All histopathological diagnoses were made according to the 2015 WHO classification for lung cancer (*24*) by at least two experienced pathologists. Tumor stage was designated according to the 7th edition of the UICC tumor, node, and metastasis (*25*). Before TMA construction, a hematoxylin and eosin (H&E)-stained slide of each block was analyzed to select tumor-containing regions. A TMA machine (AlphaMetrix Biotech, Roedermark, Germany) was used to extract two tandem 1.0-mm cylindrical core samples from each tissue donor block.

Multiplex Immunofluorescence

The multiplex immunofluorescence was performed with two different panels including either T cell related markers or macrophage related markers on formalin-fixed paraffin-embedded tissues (FFPE). The following antibodies were used: glycodelin 1:1000 (N-20, Santa Cruz Biotechnology, Dallas, TX), CD68 1:100 (PG-M1, Agilent), panCK 1:300 (AE1/AE3, Zytomed, Berlin, Germany), iNos 1:300 (SP126, Abcam, Camebridge, UK), CD8 1:100 (SP16, Abcam), CD4 1:100 (EP204, Cell Signaling Technology, Danvers, MA), Granzyme B 1:300 (D6e9W, Cell Signaling Technology). The staining procedure as well as the image analysis is described in the supplemental material. The patient cohort is characterized in Table 1. For overall survival analyses, patients with incomplete surgical resection and no detectable glycodelin staining were excluded.

Immunoblot

Glycodelin was detected using the polyclonal anti-glycodelin antibody 1:300 (N-20, Santa Cruz Biotechnology). Anti-beta-actin 1:10,000 (A5441, Merck) was used as loading control. The detailed procedure is described in the supplemental material.

Lectin-based pull-down assay

A set of eight different lectins (BK-1000, BK-3000, BK-2100, BIOZOL, Eching, Germany) was used for glycan binding studies. Biotinylated lectins were incubated with streptavidin-coupled magnetic beads (Thermo Fisher Scientific) for 45 min on the overhead shaker. Cell culture supernatants from 4950T or 170162T cells were concentrated 10x using Amicon centrifugal filtration units with 100 kDa cutoff filter (Merck). Concentrated supernatant or glycodelin A isolated from amniotic fluid was added to the lectin coupled beads and incubated overnight on an overhead shaker at 4 °C. Supernatant was collected as control and the beads were thoroughly washed 3 x with TBS/Tween 0.2% after which bound proteins were eluted by adding hot reducing SDS sample buffer containing 2-mercaptoethanol (Merck) and boiling for 5 min at 99 °C. Samples were analyzed *via* immunoblot. For each lectin, signal in control supernatant (flowthrough, FT) was compared to the signal of bound protein and scored according to the relative signal. Binding was considered was considered as strong (>70 % of the signal was detected in the bound fraction compared to the FT), moderate (40-69 % of the signal in bound fraction), weak (10-39 %), or no detectable binding (0-9 %).

Measuring of glycodelin and hormones

Glycodelin levels in serum were measured using a glycodelin ELISA from Bioserv (BS-30-20, Bioserv Diagnostics, Berlin, Germany) according to the manufacturer's instructions. Patient cohort is described in Table 1. Glycodelin concentrations in cell culture supernatants were measured using in house immunoassay (*26*).
The hormones were measured by the clinical diagnostics of the Heidelberg University Hospital. For hCG, progesterone and testosterone the ADVIA Centaur XPT system was used (Siemens Healthcare Diagnostics, Eschborn, Germany). Estrogen concentration was determined using Cobas E411 (Roche Diagnostics, Mannheim, Germany).

Table 1. Clinical parameters of the investigated patient cohorts
NOS = not otherwise specified, n.d. = no data, ECOG = Eastern Cooperative Oncology Group, mAb = monoclonal antibody, LUSC = Lung squamous cell carcinoma, LUAD = Lung adenocarcinoma, LCC = Large cell carcinoma, NOS = not otherwise specified, SCC = Small-cell lung cancer, TMA = tissue multi array

Cohort characteristics - Immunotherapy serum cohort						
Parameter	**n**	**(%)**		**Parameter**	**n**	**(%)**
Median Age	63 (38-85)			***Line Immunotherapy***		
Total	**139**			1st	77	55
				2nd	53	38
Gender				3rd	6	4
Male	81	58		4th	3	2
Female	58	42				
				mAb therapy		
Histology				PD-1	114	82
LUSC	31	22		PD-L1	25	18

LUAD	97	70				
LCC	3	2		***ECOG***		
NOS	8	6		0	57	41
				1	74	53
PD-L1				2	2	1
<1 %	24	17		n.d.	6	4
1-49 %	54	39				
>50 %	45	32				
n.d.	16	12				

Cohort characteristics – Multi IF tissue cohort (TMA)						
Parameter	**n**	**(%)**		**Parameter**	**n**	**(%)**
Median Age	63 (38-86)			***ECOG***		
Total	726			0	508	70
				1	191	26
Gender				2	25	3
Male	484	67		3	1	0
Female	242	33		4	1	0
Histology				***Pathological stage (7th edition)***		
LUSC	247	34		I	228	31
LUAD	374	52		II	192	26
NSCLC mix	45	6		III	261	36
LCC	34	5		IV	36	5
NOS	25	3		n.d.	9	1
SCC	1	0				
Smoking status						
Current smoker	209	29				
Ex-smoker	421	58				
Never smoker	72	10				
n.d.	24	3				

In vitro binding assays and antibody blocking

The cell line 4950T secretes glycodelin into the culture supernatant in high amounts compared to other cell lines (average of 100 ng/ml for confluent cells per day). For cell-based assays, cell culture supernatant was concentrated using Amicon filter columns with either 30 kDa or 100 kDa cutoff (Merck), retaining glycodelin in the concentrated part. For time course binding assays, the concentrated supernatant was diluted to the initial concentration with cell culture medium without FBS. For binding assays with deglycosylated glycodelin, the condensed supernatant was first incubated with PNGase F (Promega, Walldorf, Germany), heat-inactivated, and then diluted to the initial concentration. Deglycosylation was controlled by immunoblot. For blocking assays, unconcentrated cell culture supernatants were incubated with a rabbit monoclonal anti-glycodelin antibody (clone 12C9, kindly provided by ROCHE, Penzberg, Germany) for 1 h at room temperature prior to incubation with immune cells. 5 µg of normal rabbit IgG (source) was used as control. After treatment, cells were washed three times with PBS and boiled for 5 min at 99°C in hot reducing SDS-buffer containing 2-mercaptoethanol (Merck).

Affymetrix gene expression analysis

Control and knockdown 4950T cell culture supernatants were concentrated using an Amicon filter column with a 30 kDa cutoff and glycodelin levels were measured *via* ELISA. The supernatants were diluted to final glycodelin concentrations of 200 ng/ml (control) and 60 ng/ml (knockdown) in RPMI without FBS (+10 ng/ml IL-2 for KHYG-1 treatment). The immune cell lines Jurkat, THP1, and KHYG-1 were washed and 5 x 10^5 cells were treated with 1 ml of concentrated supernatant for 3, 8, or 24 h. Cells were collected, washed with PBS and RNA was isolated as described above.

For Affymetrix gene chip analysis, total RNA was processed following the instructions of GeneChip™ 3' IVT PLUS Reagent Kit User Guide (Manual Target Preparation for GeneChip™ 3' Expression Arrays). Chips covering the Human Genome Array Type: HG-U133_Plus_2 were prepared and used to assess the gene expression. Data were analyzed using Transcriptome Analysis Console and Ingenuity Pathway Analysis Software (Qiagen). Genes with a fold change expression of < -2 or > 2 and a p-value < 0.05 were included in subsequent analyses. Canonical pathway analysis and networks were generated using QIAGEN IPA. The microarray data were deposited into the NCBI GEO database.

Statistical analyses

Progression-free survival (PFS) data were statistically analyzed using REMARK criteria with SPSS 29.0 for Windows. The primary endpoint of the study was progression-free survival. PFS time is calculated from the date of immunotherapy until the day of diagnosed tumor progression or death. Analysis of survival data was performed using Kaplan-Meier estimator and Cox proportional hazards model. The cut-off between high and low concentrations was identified by CutOff Finder version 2.1 (*27*). For glycodelin serum analyses, the median was the optimal cut-off. Univariate significance between the groups was examined by the log-rank test. Multivariate survival analysis was performed using the Cox proportional hazards model. Mann-Whitney U test was used to investigate significant differences between non-parametric datasets (patient related data). The Spearman ranked correlation coefficient test was performed for correlation analyses. Paired t-test was applied for *in vitro* experiments with at least three biological replicates. A p-value of less than 0.05 was considered significant. Visualization of the data was made by GraphPad Prism 5 (GraphPad Software, San Diego, CA).

Results

Comparison of the glycosylation pattern of NSCLC-derived glycodelin and immunosuppressive glycodelin A

The immunosuppressive function of glycodelin A is primarily mediated by its high sialylation degree and a distinct glycosylation pattern (*28*). In order to characterize the glycosylation pattern of NSCLC-derived glycodelin, a lectin based pull-down assay was performed investigating eight different binding specificities.

For these experiments, two patient-derived NSCLC cell lines 4950T and 170162T (Fig. S1) were used. Both cell lines express the lung adenocarcinoma markers thyroid transcription factor 1 (TTF1) and cytokeratin 7 (CK7) and secrete high amounts of glycodelin. As outlined in Fig. 1A, the supernatants of the NSCLC cells were concentrated and incubated with different

lectins. The binding of glycodelin was assessed by immunoblotting (Fig. 1 A). The successful concentration of the cell culture supernatants through a centrifugal filter with a mass cutoff of 100 kDa was confirmed by the presence of glycodelin in the supernatant concentrates (Fig. 1 B). The binding of glycodelin present in the supernatants from 4950T cells (SN1) and 170162T cells (SN2) to specific lectins was compared to the binding of glycodelin AF, isolated from amniotic fluid, that was used as a control glycodelin glycoform with a known immunosuppressive function (Fig. 1 C).

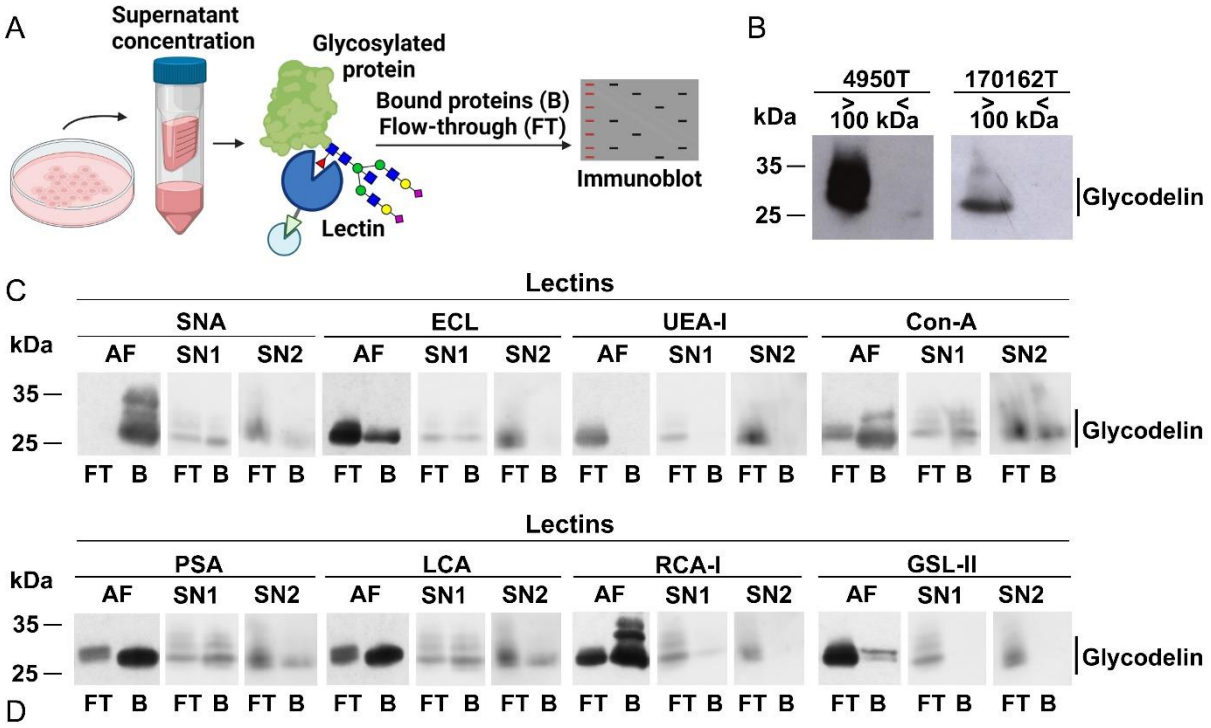

Lectin	GdA	4950T	170162T	Binding Specificity
SNA (*Sambucus nigra* agglutinin)	+++	+++	+	Neu5Acα6Gal/GalNAc
ECL (*Erythrina cristagalli* lectin)	++	++	-	Galβ4GlcNAc
UEA I (*Ulex europaeus* agglutinin)	-	-	-	αFuc
Con-A (Concanavalin A)	+++	+++	+++	αMan, αGlc
PSA (*Pisum sativum* agglutinin)	+++	+++	++	αMan, αGlc
LCA (*Lens culinaris* leucoagglutinin)	+++	+++	++	αMan, αGlc
RCA I (*Ricinus communis* agglutinin)	+++	+	-	Gal
GSL II (*Griffonia (Bandeiraea) simplicifolia* lectin II)	++	-	-	αGal

Figure 1: Comparison of the glycosylation pattern of NSCLC-derived glycodelin and glycodelin A. A) Schematic description of the experimental setup. Supernatant from cell lines 4950T and 170162T were collected, condensed, incubated with different lectins and analysed by immunoblot. B) Glycodelin in concentrate and flowtrough after concentration with a 100 kDa protein column. C) Binding capacities of glycodelin from amniotic fluid (AF), supernatant of 4950T (SN1) and 170162T (SN2) to eight different lectins. D) Evaluation of signal intensities from immunoblots shown in B). Binding specificity is based on the manufacturer's (Vector Laboratories) information. AF = glycodelin from amniotic fluid, SN1 = 4950T supernatant, SN2 = 170162T supernatant, FT = flowthrough, B = bound to lectin, GdA = glycodelin A. +++ strong binding, ++ moderate binding, + weak binding, - no binding.

The results of the immunoblotting analysis (Fig. 1 C) and the quantitative evaluation (Fig. 1 D) revealed that glycodelin present in the NSCLC cell line supernatants and immunosuppressive glycodelin A from amniotic fluid share many features. All examined glycodelins were bound by

Sambucus Nigra Agglutinin (SNA) which is specific for sialic acid, an ubiquitous carbohydrate residue in glycodelin A important for its immunosuppressive function (*29*). However, the signal for the glycodelin from the 170162T cell line supernatant was weaker compared to the glycodelin from amniotic fluid and 4950T cell line. Another difference was that 170162T derived glycodelin the lacked binding to *Erythrina cristagalli* lectin (ECL), while otherwise the glycodelins from 170162T and 4950T cell supernatants behaved similar in lectin binding assays. Glycodelin from all three sources were bound by Concanavalin-A (Con-A), *Pisum sativum* agglutinin (PSA), and *Lens culinaris* agglutinin (LCA) and thus seemed to share the typical sugar backbone consisting of mannose and glucose (*30*).

In summary, glycodelin secreted by NSCLC cell lines showed similar, but not identical, lectin binding properties to immunosuppressive glycodelin A from amniotic fluid.

Binding of NSCLC-derived glycodelin to immune cells *in vitro*

After revealing the structural similarities of the glycans of glycodelin A and NSCLC-derived glycodelin, we investigated the capability of 4950T-derived glycodelin to bind to immune cells. Hence, immortalized leukocyte cell lines Jurkat (T lymphocytes), THP1 (monocyte-derived), and KHYG-1 (natural killer cells) were incubated with glycodelin-containing cell culture supernatants from 4950T cells. Binding of glycodelin to the immune cells was analyzed by immunoblotting (Fig. 2). Time course experiments revealed rapid binding kinetics of glycodelin to the three immune cell lines (Fig. 2 A). We confirmed that the immune cells by themselves did not express glycodelin at the RNA or protein level and that glycodelin was neither detectable in the various media used for culturing of the immune cells (Suppl. Fig. 2 A).

The incubation of tumor-derived fibroblasts or of a lung squamous cell line with the supernatants of 4950T showed only poor or no binding of glycodelin supporting that binding of glycodelin is specific for immune cells (Fig. 2 B). To evaluate whether the binding of glycodelin to the immune cells is dependent on its glycosylation, we pretreated the glycodelin-containing supernatants with PNGase F to remove the glycosylation (Fig. 2 C). These studies revealed that the binding of deglycosylated glycodelin to the immune cells was at least as strong and as rapid as the binding of the glycosylated form (Suppl. Fig. 2 B) indicating that N-glycosylation of glycodelin is not essential for its binding properties. Importantly, the application of a monoclonal anti-glycodelin antibody resulted in concentration-dependent manner in a strong inhibition of glycodelin binding (Fig. 2 D-F) pointing a translational application.

In conclusion, we demonstrated for the first time that NSCLC-derived glycodelin binds to immune cells in a glycosylation-independent manner and that this binding can be blocked by a glycodelin-specific antibody.

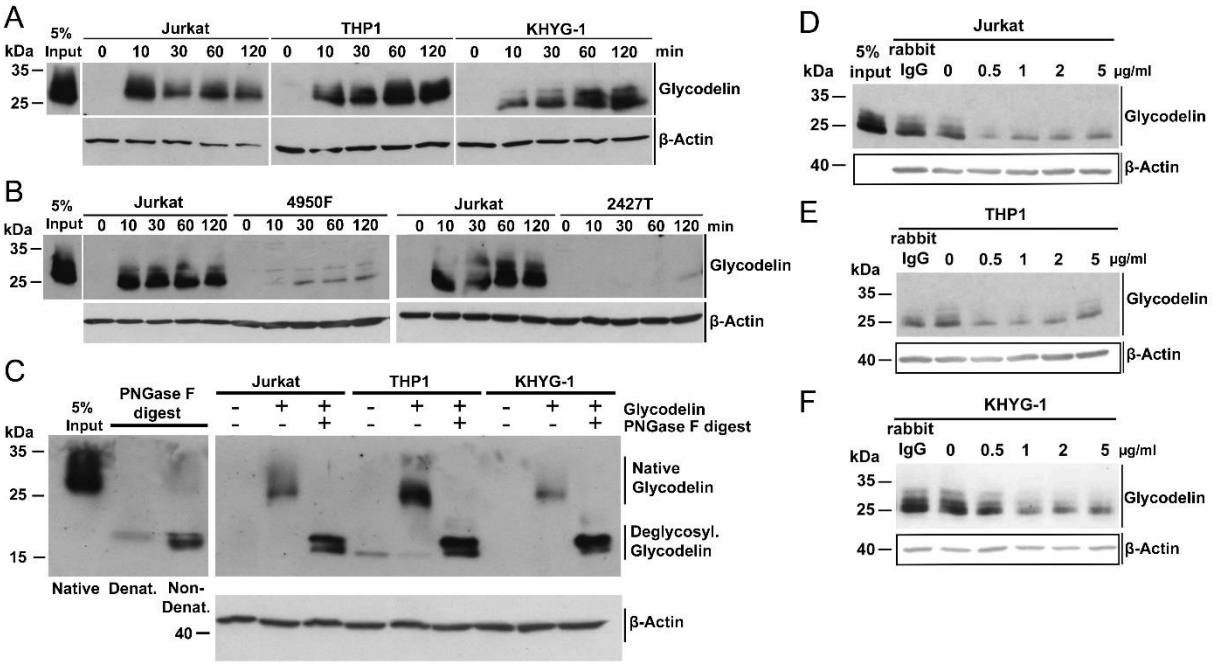

Fig. 2. Binding of NSCLC-derived glycodelin to immune cells. A) The three immune cell lines Jurkat, THP1 and KHYG-1 were incubated with glycodelin-containing supernatants from 4950T cells for the indicated time. Cells were washed with PBS to remove unbound glycodelin and lysed for immunoblot. B) A fibroblast cell line 4950F as well as a lung squamous cell carcinoma cell line2427T were incubated with glycodelin-containing supernatants from 4950T for the indicated time. C) Glycodelin from 4950T supernatant was deglycosylated by PNGase F digestion. Subsequently, the three cell lines Jurkat, THP1 and KHYG-1 were incubated with the undigested and digested supernatants. D-F) Supernatants of 4950T cells was preincubated with an anti-glycodelin antibody for 1 h with the indicated concentrations. Afterwards, Jurkat (D), THP1 (E) and KHYG-1 (F) were cultivated in these supernatants for 24 h, washed and lysed for immunoblots. A normal rabbit IgG was used as negative control. Beta-actin was used as loading control.

Impact of NSCLC derived glycodelin on gene expression in monocytic and natural killer cells

Several functions, relevant for menstruation and pregnancy, have been proposed for glycodelin A in the endometrium (*10, 15*). Numerous studies have investigated the highly pleiotropic effects and the modulation of the functionalities of different leukocytes through the interaction with glycodelin (*29-31*). In NSCLC, the function of glycodelin was not yet characterized. While glycodelin has been shown to be highly expressed in lung tumor tissue compared to normal lung (*19*), the functionality and possible immunomodulating impact remained to be resolved.

To delineate the functional impact of glycodelin on immune cells, a gene knockdown was performed in 4950T cells using small interfering RNAs (siRNAs) targeting the glycodelin encoding gene *PAEP*. The supernatants of knockdown cells were utilized to stimulate immune cells and the resulting alterations in gene expression was assessed by gene expression chip analysis (Fig. 3 A). As demonstrated in Fig. 3 B, the knockdown efficiency increased with higher siRNA concentrations but also led to a reduced cell viability (Fig. S3 A). Therefore, to exclude a bias due to a lower cell number in *PAEP* siRNA treated cells, we used the 1 nM siRNA concentration for the following experiments. The leucocyte cell lines THP1, Jurkat and KHYG-1 were cultivated with concentrated supernatants from 4950T cells treated with a

scrambled siRNA (control) or *PAEP* siRNA (Fig. S3 B) containing 200 ng/ml or 60 ng/ml glycodelin, respectively.

To characterize glycodelin-induced gene expression, the leukocytes were incubated for 3, 8, and 24 h with the supernatants of 4950T cells to cover possible early and late gene expression responses. Of note, upon cultivation in the medium of 4950T cells, the viability of KHYG-1 was reduced to 50 to 60% (Fig. S3 C). However, the viability was similar upon applying control or glycodelin siRNAs. For THP1 cells, up to 138 differentially expressed genes were observed at the three treatment time points, whereas for KHYG-1 cells, only at the 24 h time point 58 regulated genes were identified (Table S4-S7). For Jurkat cells, none of the treatments with glycodelin containing 4950T media resulted in a change of gene expression compared to media from glycodelin knockdown cells. Interestingly, several inflammation related genes were among the top upregulated genes in THP1. These included *TNF*, *CXCL10*, *CCL4*, and *ICAM1* (Fig. S3 D, Table S4-S7). In contrast, the gene *THBS1* was downregulated in most of the analyzed samples.

In KHYG-1 cells, similar to the findings in THP1 cells, genes encoding inflammation related factors such as *TNF*, *CCL4*, and *IFNG* as well as cell-cycle induction associated genes *CCNE2*, *CDC6*, or *E2F8* were differentially expressed after glycodelin treatment.

Ingenuity Pathway Analyses (IPA) were performed to decipher the effect of glycodelin on signaling pathways in the glycodelin stimulated immune cells (Fig. S3 E). In THP1 cells, expression of inflammatory pathway genes was deregulated such as the TREM1 signaling pathway or neuroinflammation signaling pathway. In addition, signaling pathways associated with the tumor microenvironment were affected in all samples and the pathway regarding the regulation of epithelial mesenchymal transition by growth factors was already influenced after 3 and 8 h of the treatment, respectively. In KHYG-1 cells, similar inflammatory pathways were influenced by the treatment with medium containing high glycodelin concentrations. High glycodelin in the medium resulted in signal changes of genes, which are part of hypercytokinemia/hyperchemokinemia in the pathogenesis of Influenza and the neuroinflammation signaling pathway. Furthermore, a cell-to-cell interaction pathway between dendritic cells and natural killer cells and a cell-cycle related pathway were affected.

A transcriptional network analysis revealed that the tumor necrosis factor (TNF) is at the center of the network in THP1 cells, along with additional immune response related genes (Fig. 3 C, left). The incubation of THP1 cells with medium of 4950T containing high amounts of glycodelin for 24 h resulted in gene expression changes of pathways that are important for cellular movement, immune cell trafficking, and hematological system development and function. The respective analysis of glycodelin treated KHYG-1 cells revealed changes in a major transcriptional interaction network that is important in cancer, hematological, and immunological disease (Fig. 3 C, right). Again, upregulation of *TNF* and, in addition, *CCL4* are central nodes and involved in various signaling pathways.

Selected genes of interest identified from IPA analyses were validated by qPCR (Fig. 3 D and E). In both immune cell lines, *TNF* and *CXCL10* were most strongly upregulated genes after 24 h of glycodelin stimulation but also *NFKB* signaling appeared to be upregulated at earlier treatment time points.

In summary, glycodelin has a major impact on the intracellular and intercellular network in immune cells primarily through an altered gene expression of *TNF* and *CXCL10* gene expression.

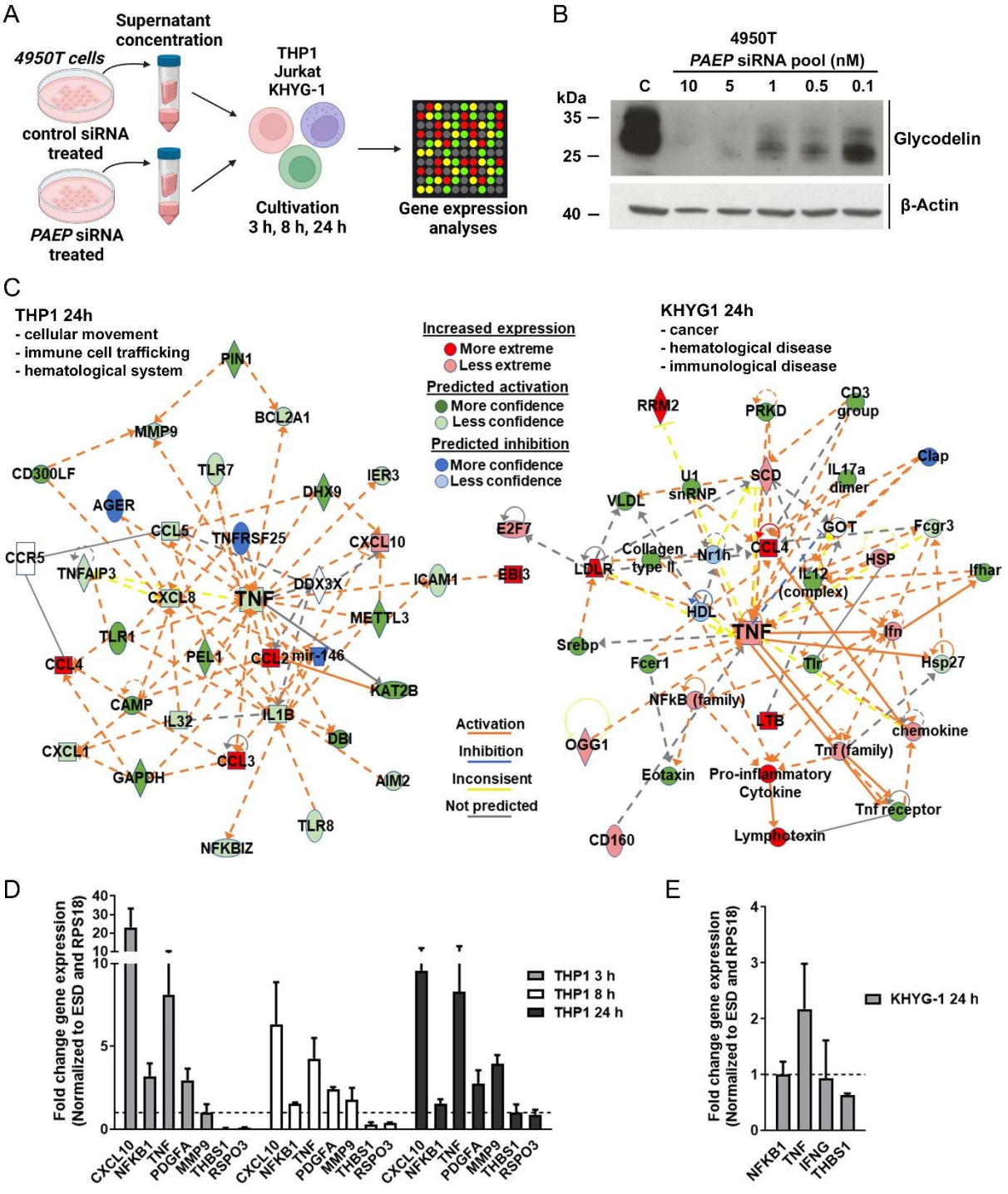

Fig. 3: Effects of cultivation of THP1 and KHYG-1 cells with glycodelin-containing supernatants. A) Schematic overview of experimental setup. Supernatants of 4950T cells treated with scrambled siRNA or PAEP siRNAs were used for THP1 cell and KHYG-1 cell incubation. Changes in gene expression were measured by gene expression chip analyses. B) 4950T cells were treated with a PAEP siRNA pool for 72 h with the indicated concentrations. Knockdown efficiency was controlled by immunoblotting. Beta-actin was examined as loading control. C) Ingenuity pathway analyses of THP1 and KHYG-1 cells after 24 h of treatment with high and low glycodelin-containing supernatants. D and E) Gene expression changes of indicated genes after treatment of THP1 cells (D) or KHYG-1 cells (E) with 4950T cell supernatants were determined by qPCR with three biological replicates each.

Spatial analysis of glycodelin and leukocyte markers in NSCLC tissue

The *in vitro* experiments revealed that glycodelin secreted by NSCLC cells carries a glycosylation pattern resembling the immunosuppressive glycosylation pattern of glycodelin A from pregnancy, is capable of binding to immune cells and affects inflammation related pathways in these cells. To validate these findings *in vivo*, we examined FFPE tissues from patients with NSCLC using multiplex immunofluorescence staining (Fig. 4). To first validate the interaction of glycodelin with immune cells in tissue sections, FFPE samples of the NSCLC patients were examined from whom the NSCLC cell lines 4950T and 170162T with known glycodelin expression were derived (Fig. 4 A). In these sections, we found glycodelin staining was mainly detected in the tumor areas but also in surrounding stroma. Here, distinct cells were detected being double positive for glycodelin and CD45 (Fig. 4 A, white arrows).

To gain comprehensive insights into the properties of glycodelin in NSCLC regarding the interaction with immune cells, spatial analysis was performed on 12 tissue microarrays (TMAs) covering 726 patients harboring NSCLC. The TMAs were stained with two different 5-plex panels and DAPI for cell nuclei staining (Fig. 4 B). In line with the previous findings, glycodelin staining in tumor and stroma was heterogenous (Fig. 4 C). panCK+ cells were mainly found in the tumors while immune cells were predominantly detected in stroma. As expected, most of the glycodelin signal found in the tumor tissue was overlapping with panCK staining (Fig. S4 A and B). When comparing CD8+/glycodelin+ double positive cells with CD4+/glycodelin+ cells, we found a strong association between glycodelin and CD8+ cells but not CD4+ cells, neither in the tumor nor in stroma (Fig. 4 D). Unfortunately, the number of Granzyme B single or double positive cells was too low for additional analyses. A large proportion of tissue punches was positive for iNOS, a M1 macrophage marker, in the tumor region, whereas the majority of CD163+ M2 macrophages were situated in the stroma (Fig. 4 E). CD68+ macrophages were detected in both areas, preferentially in the surrounding stroma. Cells triple positive for CD163, glycodelin, and CD68 were detected significantly less than cells that were only positive for CD163 and glycodelin. Cells double positive for glycodelin and iNOS could be rarely detected, regardless of the tissue regions.

In a Spearman correlation analyses we observed a medium correlation ($r = 0.51$) between the CD8+ and glycodelin+ cells in the stroma and a trend ($r = 0.4$) in the tumors of the same patients (Fig. 4 F and Fig. S4 C). The combination of glycodelin and CD163 in the stroma showed a positive correlation ($r = 0.47$, Fig. 4 G) at a similar level also to CD68+ cells in the stroma (Fig. S4 J). In contrast, cells positive for iNOS or glycodelin revealed a weakly negative correlation in the tumor with $r = -0.37$ (Fig. 4 H). None of the other markers correlated with glycodelin (Fig. S4 D-K).

The spatial analysis of the TMAs enabled a statistically robust insight into the interaction of glycodelin and different subsets of macrophages. Glycodelin seems to primarily bind to M2 macrophages, while it is mostly absent in M1 macrophages.

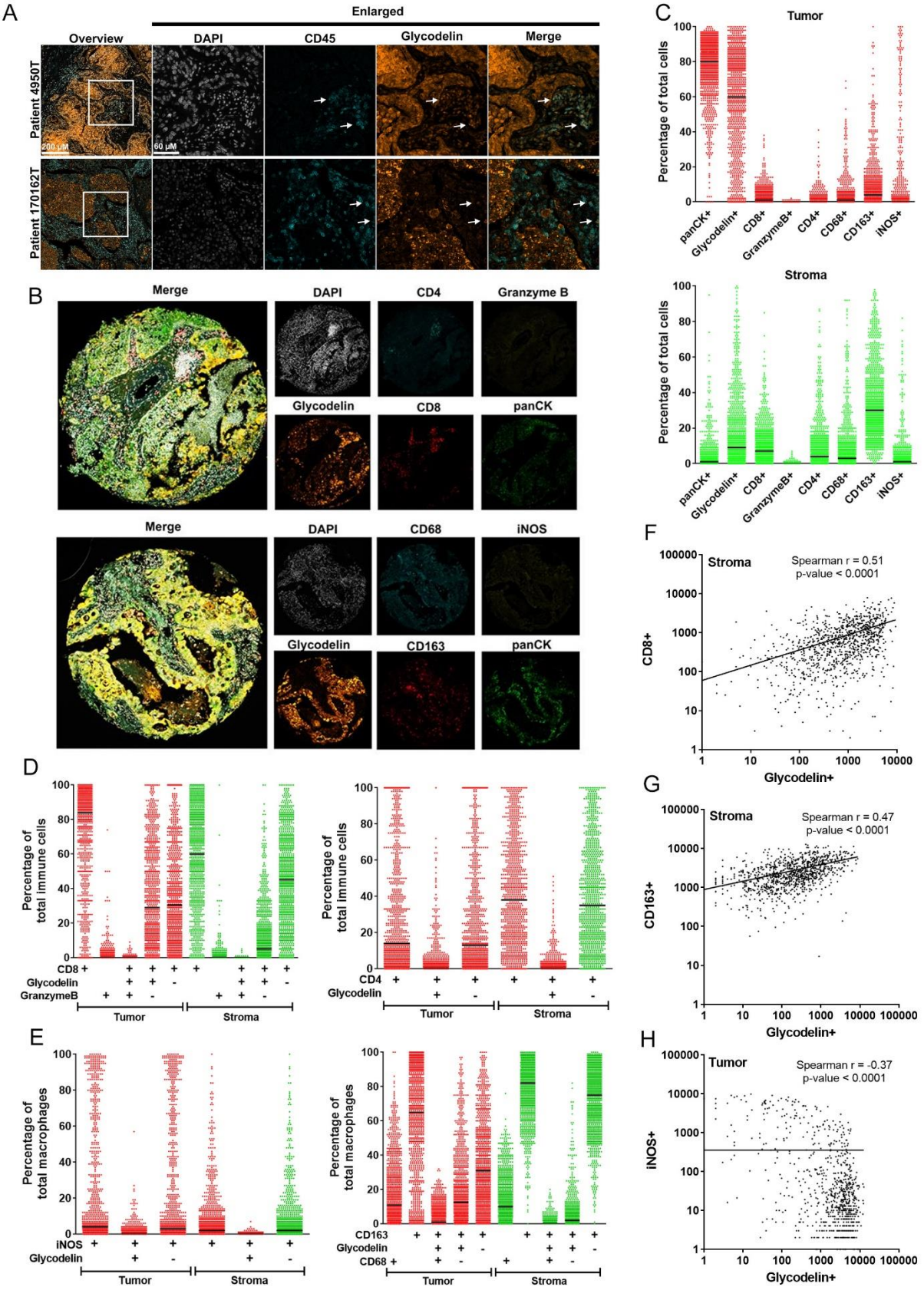

Fig. 4. Spatial analyses of glycodelin binding to immune cells *in vivo*. A) Colocalization studies of CD45+ cells and glycodelin in the tumors of 4950T and 170162T. White arrows indicate colocalizing signals. B) Representative stainings for glycodelin and a T cell marker panel as well as a macrophage panel. C) Percentage distribution of the different cell types in tumor and stroma. D) Percentage of single, double and triple positive cells in tumor and stroma for glycodelin and the indicated T cell markers. E) Percentage of single, double and triple positive cells in tumor and stroma for glycodelin and the indicated

macrophage markers. F)-H) Spearman correlation analyses of glycodelin and CD8+ cells (F), CD163+ cells (G) and iNOS+ cells (H) in tumor and stroma, respectively. P-value < 0.05 was considered significant. R > 0.5 was considered as correlation.

Based on the multi-immunofluorescence stainings, we investigated the influence of the detection of glycodelin and the co-localization with immune cells on the overall survival of the patients (Fig. 5). As already observed at the RNA level in previously published data (*19*), higher glycodelin levels in the stroma (Fig. 5 A) or in the tumor (Fig. 5 B) area were generally correlated with a worse overall survival prognosis. Both, male and female patients with a higher staining of glycodelin in the stroma showed a worse overall survival prognosis (Fig. S5 A and B). In the tumor area, glycodelin staining was prognostic only for the survival of female patients (Fig. S5 C) while the glycodelin staining in male patients (Fig. S5 D) showed no differences in relation to overall survival. We also investigated the overall survival prognosis based on our findings of a potential binding of glycodelin to M1 and M2 macrophages. While the co-localization of glycodelin and the M1 macrophage marker iNOS in the stroma correlated with in a significantly better survival prognosis (Fig. 5 C), the opposite effect was found for the co-localization of glycodelin and CD163, a M2 macrophage marker (Fig. 5 D). The analyses in the tumor area showed similar results (Fig. 5 E and F). However, generally, the correlation of the staining with the overall survival prognosis was higher in the tumor stroma compared to tumor itself. The potential binding of glycodelin to CD8+ cells was connected with a worse prognosis (Fig. S5 E+F).

In summary, the colocalization analyses and the correlation with overall survival supported that the expression of glycodelin and the binding to immune cells have a high impact on the overall survival prognosis of patients with NSCLC.

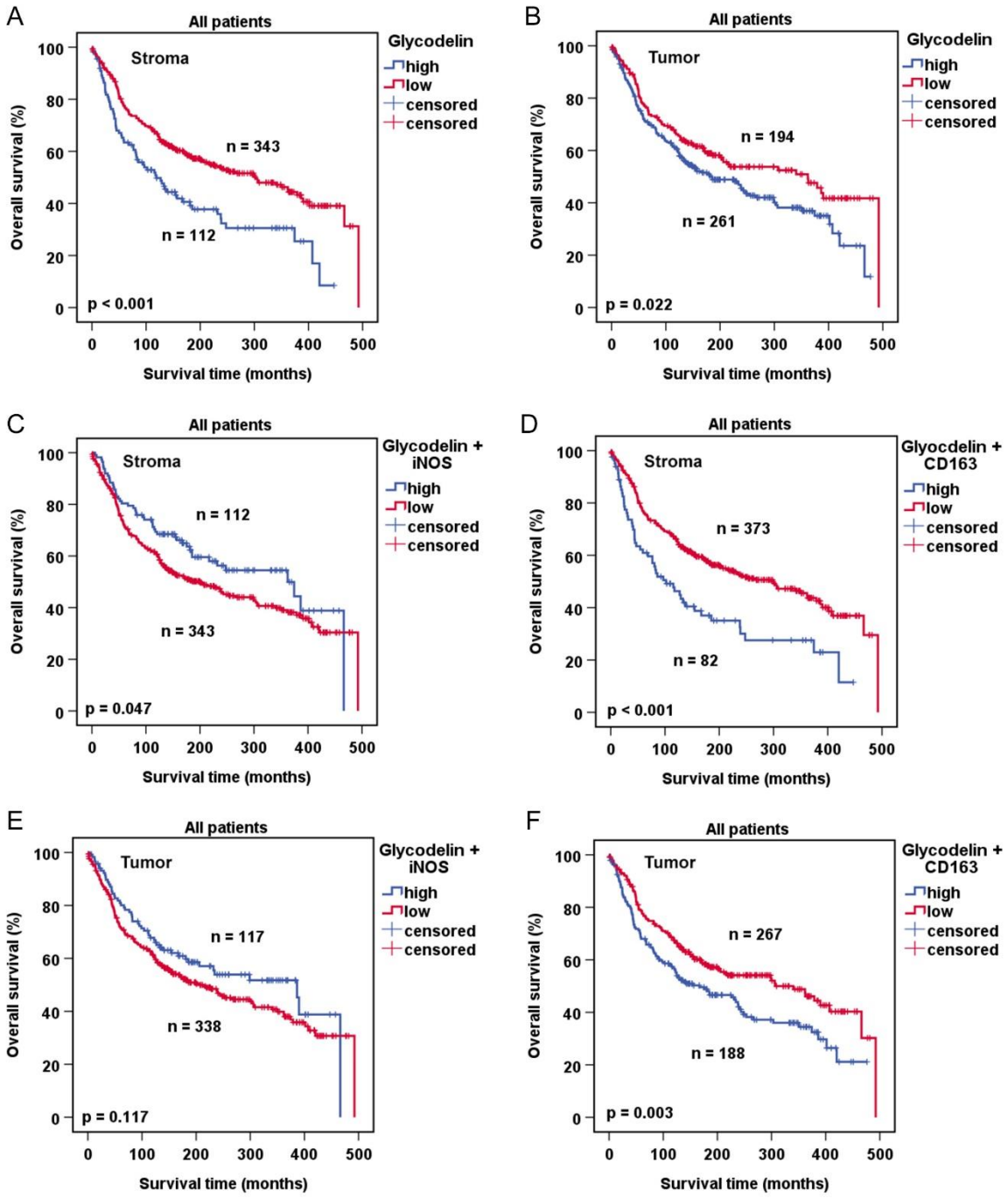

Fig. 5: Influence of glycodelin and the colocalization to immune cells on overall survival of patients. A-F. Overall survival analyses based on the multi IF stainings from Fig. 4. Cut-offs for Kaplan-Meier plots were calculated using the Cutoff-Finder (*27*). p<0.05 was considered significant.

Glycodelin serum levels predict the clinical benefit of PD-1/PD-L1 therapy in female patients

Immunotherapy for inoperable patients (stage IIIB/IV) with NSCLC is a novel approach that has led to improved treatment outcomes and prolonged progression-free and overall survival in many patients. However, several patients do not benefit from this costly treatment option (*4*).

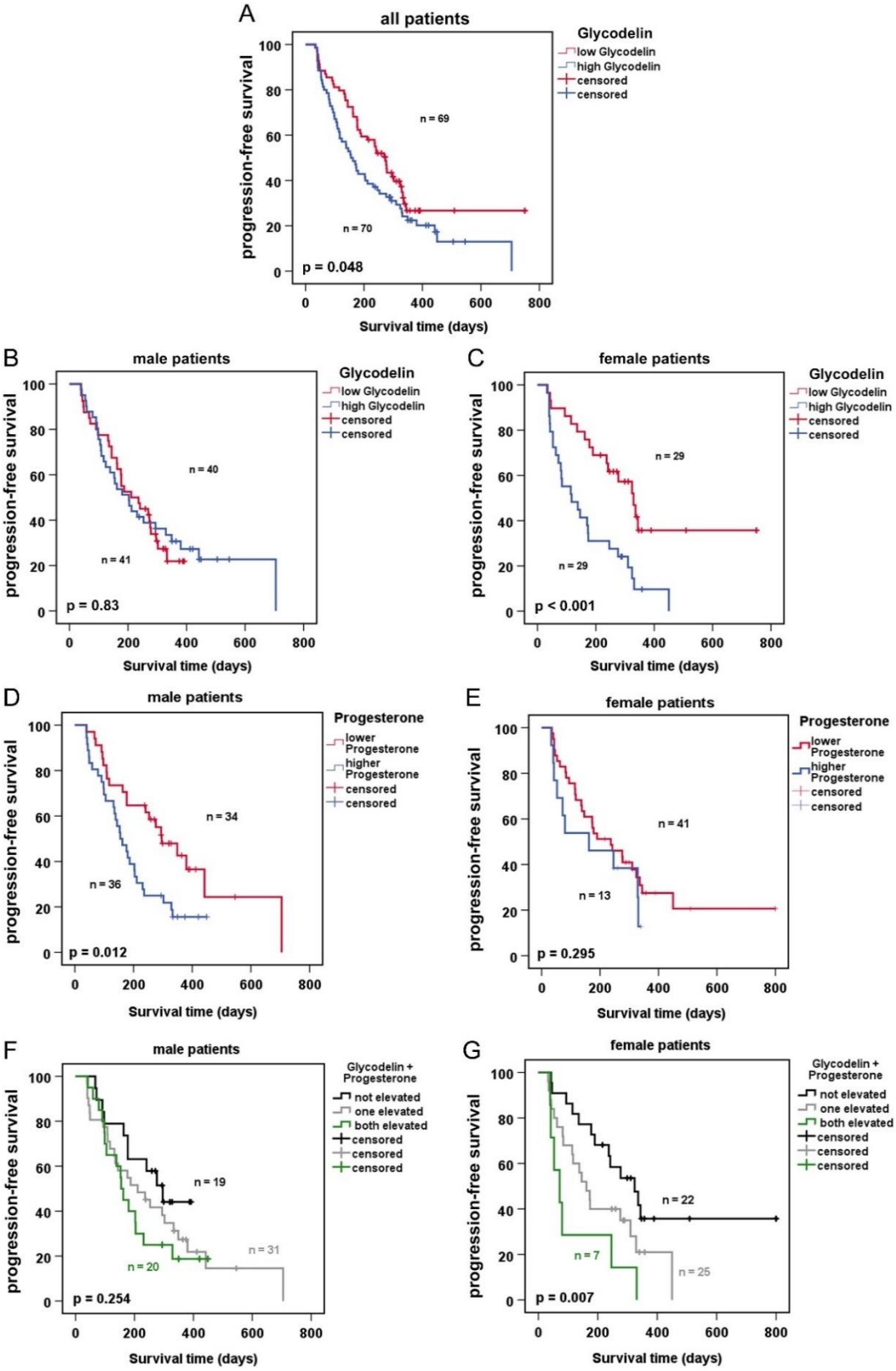

Figure 6: Associations of glycodelin and progesterone serum levels with progression-free survival (PFS) of patients receiving immunotherapy. A) – C) Kaplan-Meier plots using median glycodelin serum levels to divide patients groups. D) and E) Kaplan-Meier plots using median progesterone serum levels to divide patients in two groups. F) and G) Kaplan-Meier plots combining results from measured glycodelin and progesterone serum levels. Patients were devided in a group with

both marker values below median, one marker elevated or both values above the median. $P < 0.05$ was considered significant.

As we postulate that glycodelin regulates the tumor microenvironment by binding to immune cells (*32*), we investigated whether glycodelin serum levels correlate with progression-free survival (PFS) upon immunotherapy. All patients in the study were diagnosed with inoperable NSCLC at the time point of investigation and were treated with anti-PD-1 or anti-PD-L1 antibodies (Table 1).

During pregnancy, the level of glycodelin in the serum peaks with 2 µg/ml and reaches concentrations of over 200 µg/ml in amniotic fluid (*33*). However, in patients with NSCLC, we observed that the glycodelin serum concentrations varies widely before, ranging from 0 to nearly 300 ng/ml. Survival analyses revealed that high glycodelin serum concentrations (above median) are associated with significantly shortened PFS in all patients ($p = 0.048$, Fig. 6 A). However, this observation was not observed in male patients but only in female patients, in whom elevated glycodelin levels were associated with a significantly shorter PFS ($p < 0.001$, Fig. 6 B and C). Several studies have shown that hormones, such as progesterone, regulate glycodelin expression (*34, 35*). To investigate a potential correlation of these hormones with glycodelin expression in patients with NSCLC, the same patient samples were analyzed for serum concentrations of progesterone, testosterone, estrogen and hCG (Figure S6 A). hCG was measurable in only 39 out of the 125 patients including some with elevated levels up to 11 pg/ml. Testosterone was the only hormone that had no measured levels outside the physiological range with regards to gender-specific expression. Spearman correlation analysis did not reveal any relation between glycodelin and the investigated hormones (Fig. S6 B). Progesterone was the only hormone that was associated with poor outcome when elevated in the serum of patients with NSCLC (Fig. S6 C). This observation was restricted to male patients only (Fig. 6 D) whereas no progesterone-level dependent difference in PFS was found in female patients (Fig. 6 E).

In multivariate Cox regression analysis (Table S8) controlling glycodelin and relevant clinical parameters, progesterone turned out to be the only independent prognostic factor for PFS ($p = 0.026$) with an increased hazard ratio (HR = 1.694, CI 1.066-2.692) in the investigated cohort. A combination of glycodelin and progesterone serum levels as a 2-marker-panel was not suitable for male patients (Fig. 6 F) but significant for PFS of female patients ($p = 0.007$, Fig. 6 G). Nevertheless, the combined panel of both markers failed to exceed glycodelin's potential as biomarker alone ($p < 0.001$, Fig. 6 C).

To conclude, the patient data demonstrated that glycodelin serum levels are associated with poor progression-free survival prognosis in female patients under immunotherapy.

Discussion

Lung cancer treatment has undergone enormous improvements after the first applications of monoclonal antibodies that target the PD-1/PD-L1 axis (*36-38*). Nevertheless, overall survival for patients diagnosed at advanced stages remains poor, and there is an unmet clinical need for effective biomarkers and new targets. To address this, we studied glycodelin, which is a reproduction-related, immunosuppressive glycoprotein, expressed also in lung cancer (*15, 19, 20, 39*).

Since the functionality of the major pregnancy-associated glycodelin glycoform is dependent on its N-linked glycans, we started by characterizing of the glycan epitopes of NSCLC-derived glycodelin. This revealed significant similarities between the glycans of glycodelin A and NSCLC-derived glycodelin, although also some differences were observed. Furthermore, glycodelin secreted by 4950T cancer cells was sialylated, as detected by binding to the SNA lectin. Such sialylation has been reported to be a driver of immunomodulatory functions of glycodelin A (*15, 21, 32, 40, 41*). Therefore, our results lead to the assumption that glycodelin in NSCLC can potentially act in a similar way as glycodelin A. However, we investigated only glycodelin from two patient-derived cell lines. In future, this finding needs to be validated using patient samples.

To investigate the binding of glycodelin to immune cells, we cultivated immortalized immune cell lines with the cell culture supernatant of the NSCLC cell line 4950T as it secretes the highest amount of the protein compared to any other cell line used in our laboratory. We observed a glycosylation-independent binding of glycodelin to immune cells, but not to a control epithelial tumor cell line or a fibroblastic cell line. Moreover, preincubation of glycodelin-containing supernatants with an inhibitory antibody resulted in a highly decreased binding to immune cells. Several leukocyte specific receptors have shown to directly bind or modulate binding of pregnancy-related glycodelin, i.e. CD45, CD7, Siglec-6, or L-selectin (*42-45*). However, to identify specific receptor(s) was not in the focus of our study since we were able to block the binding to different immune cells efficiently by a glycodelin-specific antibody.

To further examine whether the interaction of NSCLC-derived glycodelin with immune cells is connected to a functional response, we treated the samples with control and glycodelin knockdown cell culture supernatant of 4950T cells. Significant genetic changes were detected in THP1 after 3, 8, and 24 h and in KHYG-1 after 24 h, between the cells incubated with media containing high or low levels of glycodelin. The glycodelin regulated genes were related to inflammatory responses and tumor microenvironment pathway. Within these, it is noteworthy that the expression of major regulators like *TNF* and *CXCL10* was increased. The role of TNF interplay between tumor and immune system is not clear since both pro- and antitumorigenic functions have been described for it (*46*). Interestingly, CXCL10 is also related to INF signaling since TNF is an inducer of CXCL10. CXCL10 has been shown to induce proliferation of tumor cells (*47*). On the other hand, recruitment of cytotoxic T cells after CXCL10 release has been observed (*48*). Of note, glycodelin A has been shown to induce apoptosis in Jurkat and THP1 cells (*30, 40*). However, we did not find hints for an induction of apoptosis pathways in our experimental setup. Taken together, previously published results, the fact that glycodelin is highly overexpressed in lung tumors and that this glycodelin-isoform interacts functionally with immune cells suggest a protumorigenic role for glycodelin in lung cancer.

The spatial analysis of glycodelin in tissue multi array from 726 patients was performed with a macrophage and a T cell marker panel to get insights into the interaction of glycodelin and the tumor microenvironment *in vivo*. The evaluation of the TMAs indicated a high proportion of glycodelin-positive CD8+ cells in the tumor and the total number of glycodelin positive cells correlated with the number of CD8+ T cells in the stroma. Since activated CD8+ T cells have effector functions and are the main targets of immune checkpoint inhibitors to reactivate an anti-tumor cytotoxic CD8+ T lymphocyte response (*49, 50*), it is possible that glycodelin, by binding to these cells, suppresses the cytotoxic activity of checkpoint inhibitors. The macrophage panel consisted of CD68 as a general macrophage marker, iNOS as an M1 macrophage marker, and CD163 representing M2 macrophages. In the investigated TMAs, glycodelin and CD163 double positive cells were found in the tumor and stroma region, while a correlation between glycodelin and CD163 M2 macrophage staining was observed in tumor stroma only. In contrast, cell densities of glycodelin positive and iNOS positive M1 macrophages showed a tendency of a negative correlation in tumor sites. While M1

macrophages have been shown to be highly important in the recognition and destruction of cancer cells, M2 macrophages are considered to support tumor growth and metastasis (*51, 52*). The results indicate an interaction of glycodelin with macrophages. The interaction may drive macrophages towards a M2-like state, and thus, modulate the tumor environment towards an anti-inflammatory and pro-tumorigenic surrounding.

The survival analyses based on the spatial profiles confirmed previous data we have published on RNA level (*19*). In general, a higher glycodelin protein expression in tumor and stroma tissue resulted in a worse overall survival prognosis for the patients. However, in the tumor, the worse prognosis is restricted to female patients only and in line with our previously published data (*19*). Moreover, the co-localization and potential binding of glycodelin to immune cells led to a shorter overall survival for the patients when glycodelin is co-localized to CD8+ cells and M2 macrophages. In contrast, binding to M1 macrophages are beneficial for the survival prognosis of the patients. Though, we rarely found iNOS positive cells in the samples supporting the hypothesis that glycodelin secretion from the tumor cells might reorganize the tumor microenvironment to form a pro-tumorigenic niche.

Immune checkpoint inhibition (ICI) represents a promising treatment option for patients with advanced NSCLC (*53*). The stimulation of coinhibitory pathways modulates the strength and duration of T cell mediated immune responses and prevents damage due to hyperinflammation. These regulatory pathways are exploited by cancer cells to overcome immune surveillance (*54*). In cell culture experiments an association between glycodelin and PD-L1 expression has already been shown (*19*). To study the association of glycodelin in therapeutic response to ICI, we measured glycodelin serum levels in patients with stage IIIB/IV NSCLC. It was found that elevated glycodelin concentrations are associated with poor outcome but only in female patients. Sex differences in drug-response have been reported regarding the benefit of female patients when treated with EGFR tyrosine kinase inhibitors (TKIs) (*55*). With regard to ICI, contradictory results have been reported (*56, 57*). Additional factors that influence a therapeutic response also include patient characteristics like ethnicity, body mass index (BMI) or the disease-context (*58*). Investigating differences between female smokers and never-smokers, we observed an increased glycodelin expression in the group of female smokers (*59*). Consideration of gender as a factor in the application of best possible treatment is still rare in current practice and may need to be considered more in future clinical trials (*60, 61*). During pregnancy, the expression of the glycoprotein is regulated by different hormones, including progesterone and hCG (*9, 35*). None of the hormones was correlated with glycodelin concentrations but progesterone levels were negatively associated with the PFS of the male patients. Progesterone interacts with specific progesterone receptors. Studies referring to the receptor functions in the lung (cancer) show contrary results and need to be further investigated (*62, 63*). At the tumor site, locally elevated amounts of specific hormones, cytokines or other regulators might influence the function of glycodelin and lead to the significant deterioration of ICI treatment in female patients.

Conclusions

Taken together, glycodelin in NSCLC interacts with specific subsets of immune cells in NSCLC tumor tissue and the surrounding stroma. We demonstrated that glycodelin might serve as an easily accessible independent biomarker to predict progression-free survival and may functionally adapt treatment options. However, it is not yet clear why elevated levels are associated with poor therapeutic response to immune checkpoint inhibitors in female patients. Future experiments are needed to further characterize the interaction of glycodelin and patient-derived immune cells and evaluate the potential of glycodelin-inhibitory antibodies alone or in combination with immune checkpoint inhibitors as a treatment option for patients with NSCLC.

Supplemental Material

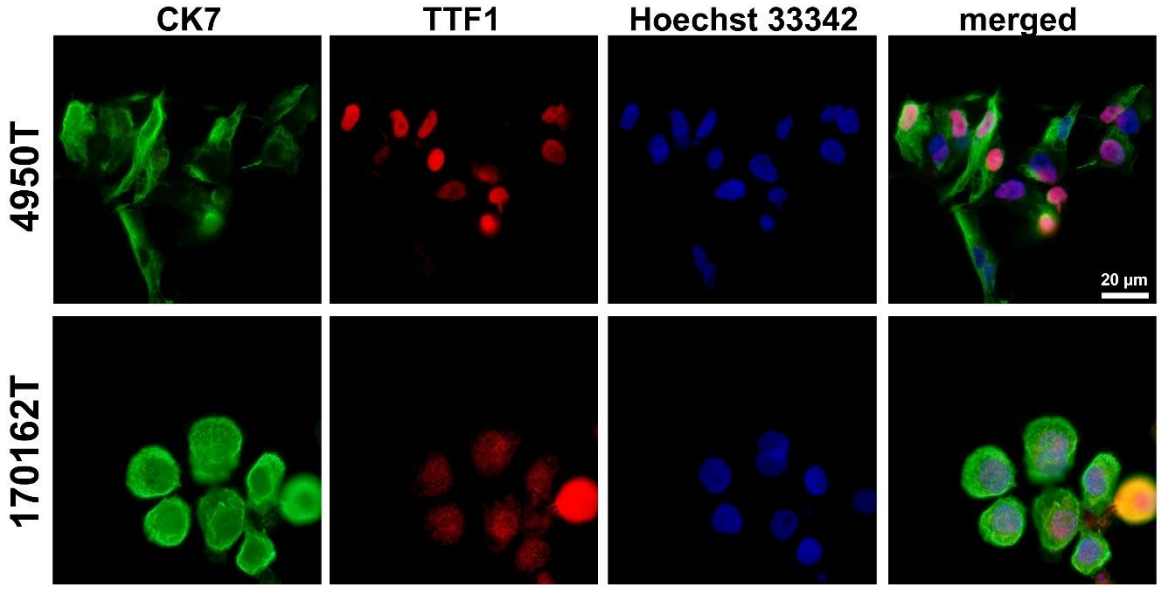

Figure S1: Characterization of 170162T cells and 4950T cells by immunofluorescence analyses. Both cell lines were stained for adenocarcinoma specific markers cytokeratin 7 (CK7) and thyroid transcription factor 1 (TTF1)

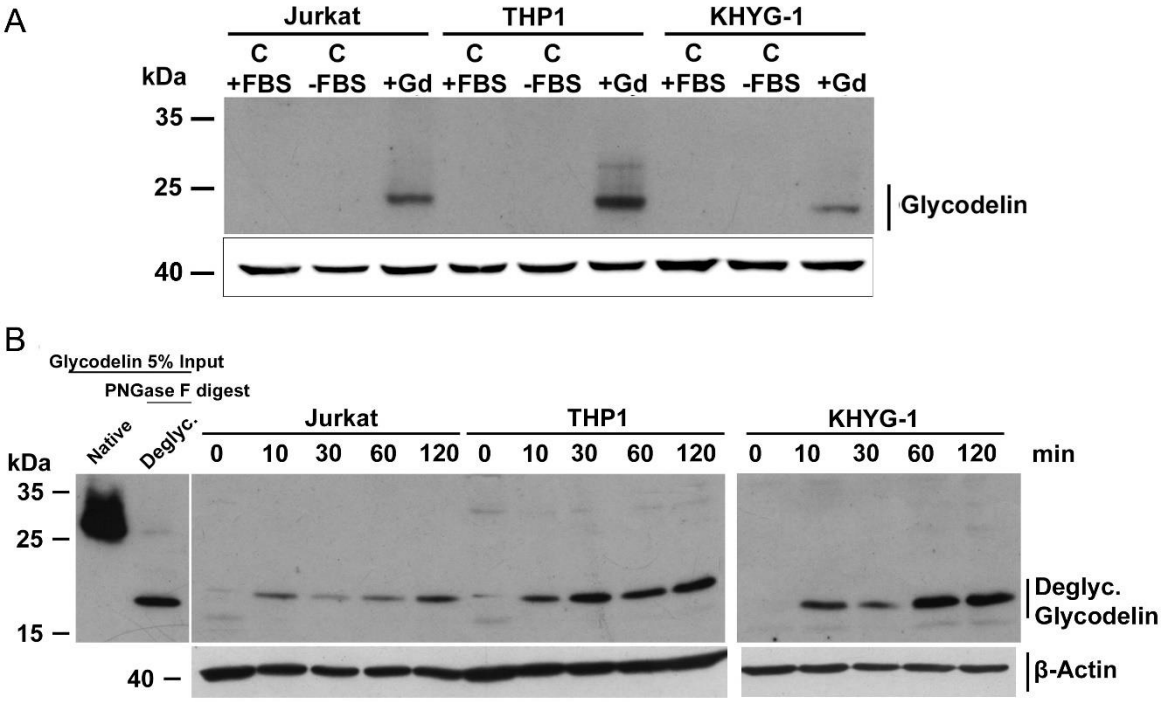

Figure S2: Binding of glycodelin to cancer immune cell lines. A) Jurkat cells, THP1 cells and KHYG-1 cells were incubated with FBS containing medium, with 4950T cell specific medium and with 4950T cell supernatants containing glycodelin for 24 h. Afterwards, cell lysates were used for immunoblot analyses. B) Time course of binding of deglycosylated glycodelin to the three investigated cell lines. Glycodelin was deglycosylated by digesting with PNGase F. Beta-actin was used as loading control.

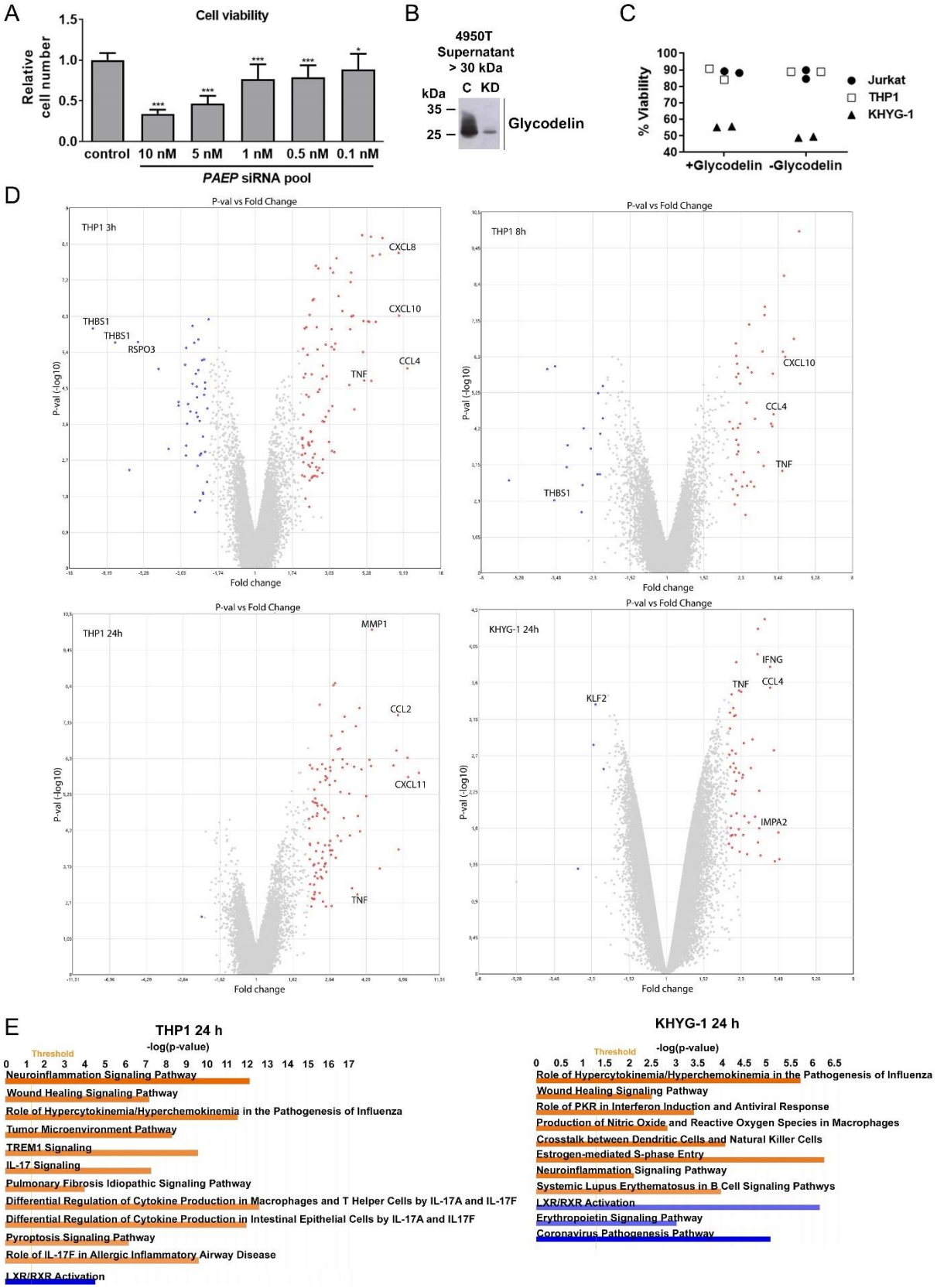

Figure S3: Differentially expressed genes and pathway of THP1 cells and KHYG-1 cells treated with glycodelin. A) Effect of *PAEP* siRNA-treatment on viability of 4950T cells using increasing *PAEP* siRNA concentrations. B) Supernatants of 4950T cells treated with scrambled siRNA (control) or *PAEP* siRNAs used for THP1 cell and KHYG-1 cell incubation. Supernatants derived from 4950T cells were concentrated using a 30 kDa cutoff filter. C) Viability of immune cells after cultivation with 4950T-derived cell supernatants for 24 h. D) Volcano plots of differentially expressed genes in both cell lines after treatment of glycodelin. Cells were incubated with glycodelin-containing or depleted supernatant from

4950T cells for the indicated time. Exemplary genes are highlighted in red if upregulated and in blue if downregulated. E) Transcriptome Analysis of the 24 h treatment of THP1 cells and KHYG-1 cells. Upregulated pathways are highlighted in orange, downregulated pathways in blue.

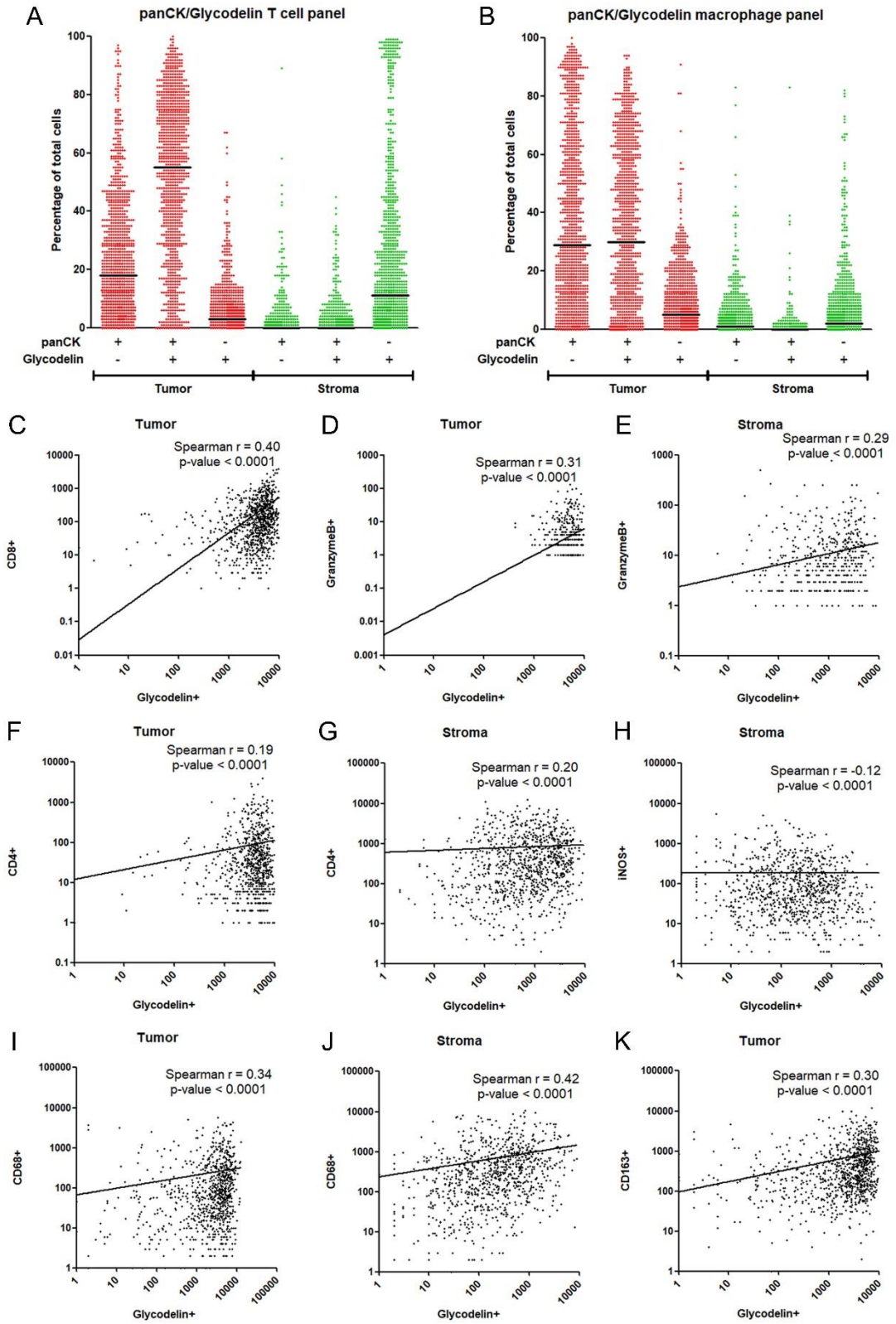

Figure S4. Multiplex IF and correlation analyses. A) and B) Percentage of single and double positive cells in tumor and stroma for glycodelin and panCK in the T cell and macrophage panel. C-K) Spearman correlation analyses of glycodelin and indicated immune cell markers. P-value < 0.05 was considered significant. R > 0.5 was considered as correlation.

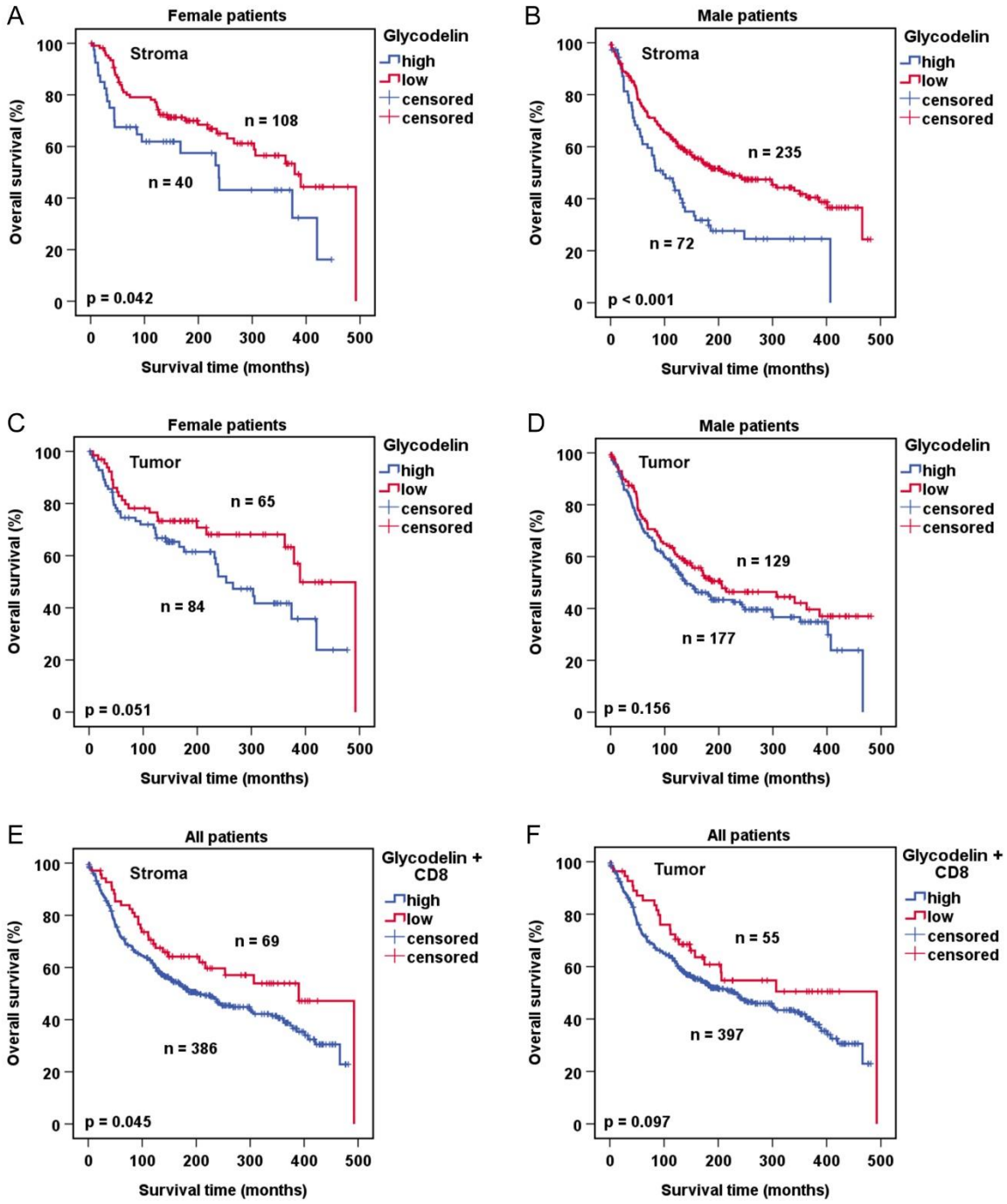

Figure S5. Overall survival analyses. A-F. Additional overall survival analyses based on the multi IF stainings from Fig. 4. Cut-offs for Kaplan-Meier plots were calculated using the Cutoff-Finder (*27*). $p<0.05$ was considered significant.

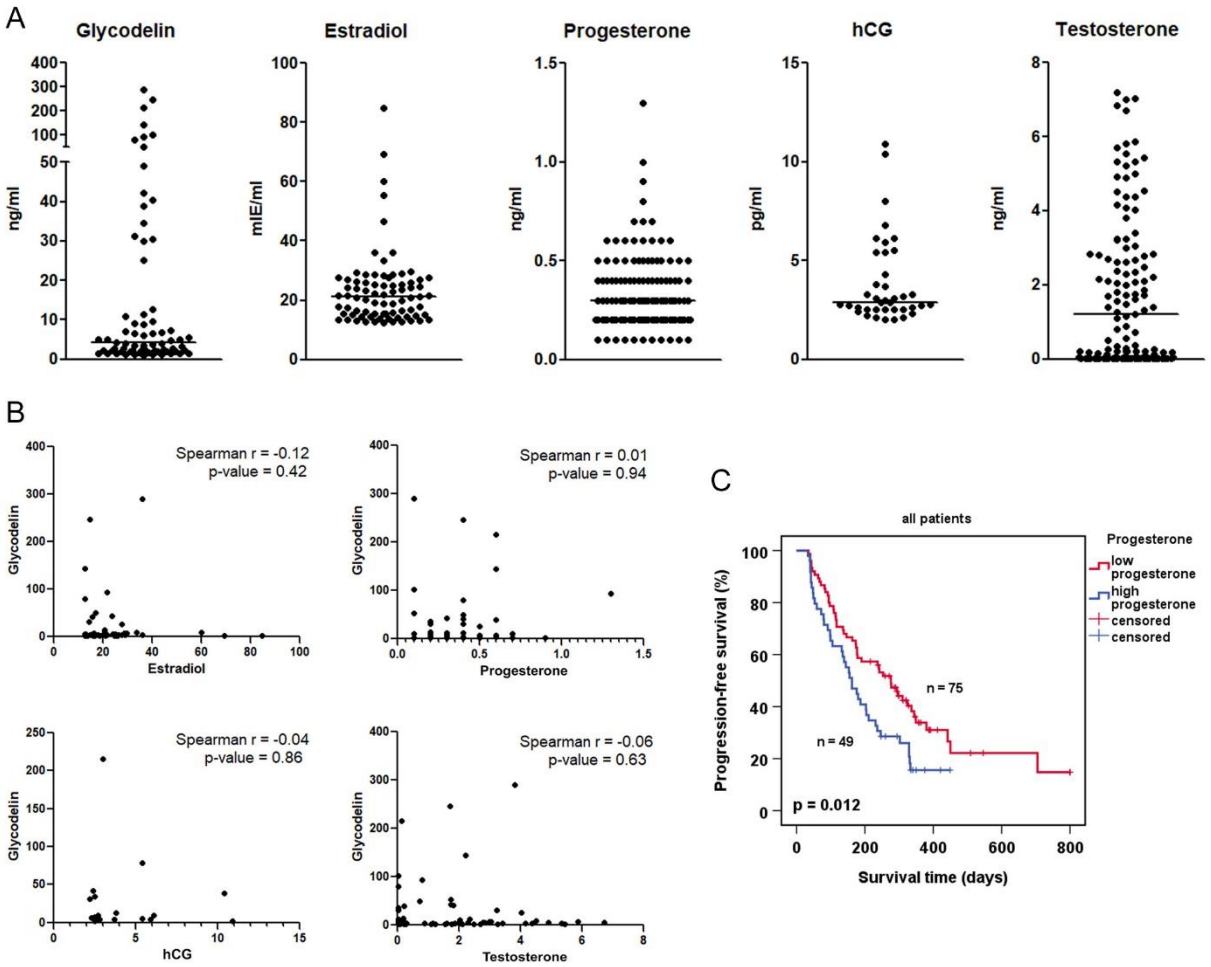

Figure S6: Analyses of hormone serum levels. A) Measured serum levels of the indicated hormones in the immunotherapy cohort (Table 1). B) Correlation between glycodelin serum concentrations and the indicated hormones. C) Progression-free survival of patients receiving immunotherapy in dependency of progesterone. Median serum concentration was used to separate the two groups.

Table S1. List of siRNAs

Name	Manufacturer	Catalog No.
AllStars Negative Control siRNA	Qiagen	SI03650318
Hs_PAEP_1	Qiagen	SI00039704
Hs_PAEP_2	Qiagen	SI00039711
Hs_PAEP_3	Qiagen	SI00039718
Hs_PAEP_5	Qiagen	SI03102659

Table S2. List of primers and probes from UPL system (ROCHE)

*The UPL system was available until December 2020. The indicated primers were used with a probe provided by the assay design center from Sigma-Aldrich Oligoarchitect™.

Name	Primer sequence 5'-3'	UPL #
ESD_for	TCAGTCTGCTTCAGAACATGG	50
ESD_rev	CCTTTAATATTGCAGCCACGA	50
RPS18_for	CTTCCACAGGAGGCCTACAC	46
RPS18_rev	CGCAAAATATGCTGGAACTTT	46
PAEP_for	CCTGTTTCTCTGCCTACAGGA	77
PAEP_rev	CGTCCTCCACCAGGACTCT	77
CXCL10_for	GAAAGCAGTTAGCAAGGAAAGGT	34

CXCL10_rev	GACATATACTCCATGTAGGGAAGTGA	34
NFKB_for	CCTGGAACCACGCCTCTA	49
NFKB_rev	GGCTCATATGGTTTCCCATTTA	49
TNF_for	CAGCCTCTTCTCCTTCCTGAT	29
TNF_rev	GCCAGAGGGCTGATTAGAGA	29
PDGFA_for	GATGAGGACCTTGGCTTGC	68
PDGFA_rev	CCAGCCTCTCGATCACCTC	68
THBS1_for	GCAGGAAGACTATGACAA	*
THBS1_rev	CTGTCATCTGGAATTTTATCA	*
MMP9_for	GAACCAATCTCACCGACAGG	21
MMP9_rev	GCCACCCGAGTGTAACCATA	21

Table S3. OPAL TSA-Fluorophores with respective protein.

Fluorophore	Macrophage panel	T cell panel
520	CD68	CD4
570	iNOS	Granzyme B
620	Glycodelin	Glycodelin
690	CD163	CD8
780	panCK	panCK

Table S4. Most regulated genes in THP1 after 3h

ID	Glycodelin Avg (log2)	no Glycodelin Avg (log2)	Fold Change	P-val	FDR P-val	Gene Symbol
204103_at	7,76	4,48	9,71	1,01E-05	0,009	CCL4
204533_at	7,43	4,33	8,56	4,84E-07	0,0013	CXCL10
202859_x_at	8,01	4,92	8,52	1,31E-08	0,0001	CXCL8
202643_s_at	9,11	6,37	6,68	5,48E-09	9,98E-05	TNFAIP3
202644_s_at	10,58	7,9	6,43	1,44E-08	0,0001	TNFAIP3
206765_at	6,35	3,75	6,06	6,89E-07	0,0015	KCNJ2
221477_s_at	9,66	7,13	5,77	1,52E-08	0,0001	LOC100129518; SOD2
211506_s_at	6,54	4,03	5,66	2,07E-05	0,013	CXCL8
1566342_at	10,14	7,65	5,63	5,15E-09	9,98E-05	SOD2
232504_at	5,78	3,33	5,49	6,95E-07	0,0015	LOC285628
205114_s_at	8,36	5,93	5,4	6,69E-07	0,0015	CCL3; CCL3L1; CCL3L3
207113_s_at	10,08	7,73	5,09	2,04E-05	0,0129	TNF
206026_s_at	5,29	2,95	5,04	6,50E-07	0,0015	TNFAIP6
206157_at	7,22	4,89	5	3,87E-06	0,0044	PTX3
202638_s_at	6,89	4,59	4,95	4,64E-09	9,98E-05	ICAM1
238727_at	5,87	3,73	4,4	0,0001	0,0393	
231779_at	8,6	6,5	4,31	4,78E-07	0,0013	IRAK2
231513_at	5,5	3,43	4,2	5,01E-07	0,0013	
204897_at	10,82	8,75	4,18	4,11E-08	0,0002	PTGER4
210538_s_at	5,45	3,4	4,16	7,11E-08	0,0003	BIRC3
236982_at	6,93	4,89	4,12	1,05E-06	0,0018	
206025_s_at	5,66	3,63	4,07	2,59E-05	0,0154	TNFAIP6
210260_s_at	9,12	7,25	3,66	3,68E-07	0,0012	TNFAIP8
215223_s_at	9,43	7,63	3,48	1,58E-07	0,0006	LOC100129518; SOD2
209288_s_at	9,52	7,77	3,38	1,76E-08	0,0001	CDC42EP3
222162_s_at	7,23	5,51	3,3	2,42E-06	0,0035	ADAMTS1

239459_s_at	5,74	4,03	3,27	0,0013	0,1794	CYP19A1
208296_x_at	8,75	7,04	3,25	3,37E-06	0,0041	TNFAIP8
223218_s_at	8,09	6,42	3,2	4,11E-08	0,0002	NFKBIZ
244414_at	6,69	5,03	3,17	8,85E-05	0,0345	
230966_at	6,65	4,99	3,14	0,0012	0,173	IL4I1
216841_s_at	8,65	7,01	3,12	1,07E-06	0,0018	LOC100129518; SOD2
209286_at	8,43	6,78	3,12	2,92E-06	0,004	CDC42EP3
222486_s_at	5,54	3,92	3,08	3,11E-08	0,0002	ADAMTS1
239876_at	7,44	5,85	3,01	0,0007	0,1278	
1558569_at	6,43	4,85	3	0,0001	0,0419	LOC100131541
220091_at	7,73	6,2	2,9	1,58E-05	0,0114	SLC2A6
225685_at	8,78	7,27	2,86	2,54E-06	0,0036	CDC42EP3
227481_at	5,97	4,45	2,86	0,0002	0,0497	CNKSR3
242405_at	6,43	4,94	2,8	0,0002	0,0597	
219908_at	6,67	5,21	2,75	8,47E-06	0,0078	DKK2
239649_at	6,77	5,31	2,74	0,0019	0,2195	
209774_x_at	5,47	4,02	2,73	1,81E-05	0,0122	CXCL2
239460_at	6,92	5,47	2,73	0,0041	0,3377	CYP19A1
204470_at	5,39	3,95	2,73	0,0002	0,059	CXCL1
201236_s_at	9,16	7,78	2,61	3,42E-05	0,0185	BTG2
217767_at	9,03	7,65	2,6	0,0031	0,2857	C3
219951_s_at	10,16	8,8	2,57	3,20E-08	0,0002	DZANK1
236738_at	8,04	6,7	2,55	3,90E-05	0,0201	C3orf80
205681_at	7,33	5,99	2,54	0,0036	0,3128	BCL2A1
220252_x_at	9,12	7,77	2,53	3,37E-06	0,0041	CXorf21
240863_at	4,29	2,95	2,52	0,0051	0,3739	CYP19A1
209892_at	10,44	9,11	2,5	9,45E-07	0,0018	FUT4
219721_at	6,46	5,15	2,48	0,003	0,2806	
202637_s_at	6,88	5,57	2,47	2,74E-08	0,0002	ICAM1
240061_at	5,7	4,42	2,43	0,0014	0,1871	
207339_s_at	7,52	6,23	2,43	0,0049	0,3692	LTB
218810_at	8,58	7,32	2,4	1,87E-07	0,0007	ZC3H12A
230614_at	6,54	5,29	2,37	0,0017	0,2057	
227180_at	5,35	4,1	2,37	0,005	0,3704	ELOVL7
209239_at	9,38	8,14	2,36	2,02E-07	0,0007	NFKB1
205463_s_at	8,89	7,66	2,34	0,0023	0,2439	PDGFA
209906_at	9,31	8,09	2,34	0,0007	0,1247	C3AR1
204823_at	6,43	5,22	2,32	0,0055	0,394	NAV3
207535_s_at	6,66	5,44	2,32	1,41E-05	0,0107	NFKB2
203548_s_at	8,88	7,68	2,3	0,0004	0,0888	LPL
203549_s_at	8,46	7,27	2,29	0,0004	0,086	LPL
242827_x_at	6,57	5,38	2,27	0,0029	0,272	
243808_at	7,18	6	2,26	0,0063	0,4222	
209287_s_at	7,77	6,6	2,25	4,58E-07	0,0013	CDC42EP3
215078_at	3,96	2,79	2,24	0,0008	0,1419	LOC100129518; SOD2
204363_at	10,11	8,94	2,24	0,0287	0,7261	F3

228343_at	6,58	5,42	2,24	0,0009	0,1419	POU2F2
237981_at	6,21	5,06	2,22	5,25E-05	0,0243	CMYA5
205242_at	4,35	3,2	2,22	0,0008	0,1365	CXCL13
209946_at	5,51	4,36	2,21	0,0007	0,1279	VEGFC
203475_at	7,88	6,73	2,21	0,0027	0,2628	CYP19A1
204440_at	8,15	7,02	2,19	4,56E-06	0,0051	CD83
1562475_at	4,96	3,86	2,15	4,68E-05	0,0228	TEX41
204224_s_at	8,14	7,04	2,14	9,47E-07	0,0018	GCH1
242907_at	4,07	2,98	2,12	1,39E-05	0,0107	GBP2
226302_at	5,79	4,71	2,12	0,0181	0,642	ATP8B1
1570505_at	5,33	4,25	2,11	0,0013	0,1834	ABCB4
216867_s_at	8,54	7,48	2,1	0,0051	0,3739	PDGFA
209893_s_at	8,67	7,61	2,09	1,01E-06	0,0018	FUT4
229437_at	8,16	7,11	2,07	1,69E-05	0,0116	MIR155HG
211122_s_at	3,5	2,46	2,05	0,0001	0,047	CXCL11
222859_s_at	6,82	5,78	2,05	0,0022	0,2365	DAPP1
213943_at	10,35	9,32	2,05	3,21E-06	0,0041	TWIST1
228153_at	4,78	3,76	2,04	0,001	0,1512	RNF144B
218627_at	7,82	6,79	2,03	0,0005	0,109	DRAM1
229830_at	8,65	7,63	2,02	0,0008	0,1414	
239529_at	8,96	7,95	2,02	0,0048	0,3656	DCANP1; TIFAB
221143_at	6,38	5,37	2,02	0,0014	0,1911	RPA4
216060_s_at	7,79	6,78	2,01	0,0006	0,1145	DAAM1
212906_at	7,74	8,74	-2,01	5,98E-07	0,0015	GRAMD1B
202254_at	5,12	6,15	-2,05	0,0001	0,0378	SIPA1L1
210512_s_at	9,81	10,84	-2,05	0,007	0,4447	VEGFA
213258_at	4,95	6,03	-2,11	3,20E-05	0,0176	TFPI
203761_at	7,06	8,14	-2,11	0,0012	0,1774	SLA
208078_s_at	6,1	7,18	-2,12	2,27E-05	0,0139	LOC102724428; SIK1
209967_s_at	6,95	8,05	-2,14	5,99E-06	0,0064	CREM
1563357_at	2,86	3,97	-2,15	4,67E-05	0,0228	TNF
200796_s_at	7,44	8,56	-2,17	0,0138	0,5906	MCL1
210643_at	4,98	6,1	-2,18	0,0129	0,5724	TNFSF11
212977_at	4,63	5,76	-2,18	0,0005	0,1048	ACKR3
204912_at	7,03	8,17	-2,21	6,30E-06	0,0066	IL10RA
230707_at	5,48	6,64	-2,23	0,0014	0,1839	SORL1
202948_at	6	7,19	-2,28	0,0203	0,6683	IL1R1
206337_at	4,36	5,56	-2,29	0,0015	0,1927	CCR7
227646_at	3,65	4,85	-2,3	0,0002	0,057	EBF1
228499_at	7,51	8,73	-2,33	1,92E-06	0,0031	PFKFB4
217738_at	7,22	8,44	-2,34	1,12E-05	0,0095	NAMPT
211527_x_at	5,85	7,09	-2,37	0,0027	0,267	VEGFA
210772_at	4,36	5,6	-2,37	0,0002	0,0497	FPR2
236220_at	3,78	5,04	-2,39	5,38E-05	0,0247	SLC16A10
203887_s_at	10,55	11,81	-2,4	2,85E-05	0,0164	THBD
209723_at	7,54	8,81	-2,41	0,0001	0,0449	SERPINB9

203888_at	9,95	11,23	-2,43	1,36E-05	0,0107	THBD
217996_at	5,91	7,21	-2,45	0,0394	0,7817	PHLDA1
226844_at	4,18	5,5	-2,49	2,33E-06	0,0034	MOB3B
229568_at	3,68	5,03	-2,55	2,41E-05	0,0145	MOB3B
201041_s_at	6,91	8,26	-2,55	8,84E-07	0,0018	DUSP1
220330_s_at	4,49	5,88	-2,64	0,0001	0,0421	SAMSN1
205119_s_at	6,09	7,54	-2,74	7,80E-05	0,0316	FPR1
206877_at	4,73	6,2	-2,77	0,0002	0,0632	MXD1
237252_at	7,83	9,31	-2,79	3,10E-06	0,004	THBD
221009_s_at	6,36	7,84	-2,8	0,0009	0,1419	ANGPTL4
225842_at	6,24	7,73	-2,82	0,0015	0,1947	PHLDA1
226275_at	7,43	8,94	-2,85	8,12E-06	0,0078	MXD1
206118_at	5,62	7,27	-3,14	8,51E-05	0,0334	STAT4
228846_at	7,52	9,18	-3,15	6,93E-05	0,0295	MXD1
223333_s_at	5,07	6,94	-3,65	0,001	0,1585	ANGPTL4
201108_s_at	4,64	6,72	-4,23	1,03E-05	0,009	THBS1
228186_s_at	4,61	7,14	-5,78	2,21E-06	0,0034	RSPO3
205239_at	6,3	9,02	-6,57	0,0035	0,3086	AREG
201109_s_at	4,87	7,89	-8,1	2,28E-06	0,0034	THBS1
201110_s_at	5,31	8,82	-11,35	1,00E-06	0,0018	THBS1

Table S5. Most regulated genes in THP1 after 8h

ID	Glycodelin Avg (log2)	no Glycodelin Avg (log2)	Fold Change	P-val	FDR P-val	Gene Symbol
215223_s_at	9,67	7,53	4,42	1,14E-10	6,24E-06	LOC100129518; SOD2
205943_at	7,05	5	4,14	1,54E-07	0,0014	TDO2
204533_at	6,68	4,77	3,76	5,04E-07	0,0023	CXCL10
1566342_at	9,5	7,61	3,72	2,22E-09	6,06E-05	SOD2
221477_s_at	8,68	6,8	3,67	3,63E-07	0,0022	LOC100129518; SOD2
207113_s_at	8,14	6,27	3,65	0,0011	0,1675	TNF
204103_at	6,26	4,54	3,3	2,37E-05	0,0202	CCL4
219424_at	5,83	4,12	3,27	1,55E-06	0,0039	EBI3
230966_at	6,75	5,04	3,25	5,28E-05	0,0331	IL4I1
205242_at	7,4	5,72	3,21	4,55E-05	0,0311	CXCL13
216841_s_at	8,6	7,01	3	1,74E-08	0,0003	LOC100129518; SOD2
220091_at	7,67	6,09	2,98	3,04E-08	0,0004	SLC2A6
204475_at	4,68	3,12	2,95	0,0008	0,1382	MMP1
202638_s_at	6,23	4,69	2,92	3,50E-07	0,0022	ICAM1
203562_at	5,94	4,46	2,78	0,0003	0,0817	FEZ1
221159_at	5,39	3,97	2,68	3,22E-05	0,0241	
205114_s_at	7,22	5,81	2,66	0,003	0,2712	CCL3; CCL3L1; CCL3L3
212190_at	9,63	8,26	2,59	1,45E-06	0,0039	SERPINE2
239459_s_at	5,58	4,23	2,55	0,0022	0,2351	CYP19A1
211597_s_at	5,39	4,07	2,51	5,82E-08	0,0006	HOPX
232504_at	4,91	3,6	2,48	1,02E-06	0,0031	LOC285628
220146_at	4,8	3,51	2,45	0,0029	0,2652	TLR7

207819_s_at	6,66	5,37	2,44	1,10E-05	0,0127	ABCB4
209875_s_at	8,54	7,27	2,41	0,02	0,578	SPP1
209946_at	5,32	4,08	2,37	0,0012	0,1738	VEGFC
230614_at	6,44	5,22	2,32	0,0031	0,2719	
202644_s_at	9,69	8,51	2,27	3,02E-06	0,0059	TNFAIP3
211122_s_at	4,02	2,84	2,27	4,55E-05	0,0311	CXCL11
229830_at	6,96	5,81	2,23	0,0003	0,0801	
205463_s_at	7,71	6,56	2,22	0,0002	0,0649	PDGFA
231513_at	7,49	6,33	2,22	1,56E-06	0,0039	
209994_s_at	6,43	5,29	2,21	5,92E-05	0,0349	ABCB1; ABCB4
219721_at	6,51	5,37	2,2	0,0055	0,3591	
216867_s_at	7,88	6,74	2,2	0,0004	0,0886	PDGFA
228060_at	7,35	6,22	2,19	8,01E-07	0,0031	SLC35F1
219938_s_at	7,74	6,62	2,18	0,0001	0,0551	PSTPIP2
202643_s_at	8,31	7,19	2,18	4,78E-07	0,0023	TNFAIP3
203475_at	9,18	8,06	2,17	1,98E-06	0,0044	CYP19A1
207339_s_at	6,81	5,7	2,16	0,0021	0,2292	LTB
205404_at	9,57	8,46	2,16	2,05E-07	0,0016	HSD11B1
239460_at	6,62	5,53	2,14	0,0102	0,4683	CYP19A1
236471_at	4,24	3,17	2,1	0,0036	0,2919	NFE2L3
206765_at	8,15	7,09	2,09	6,20E-05	0,0349	KCNJ2
228153_at	5,02	3,98	2,06	0,0014	0,1874	RNF144B
202748_at	6,05	5,03	2,02	3,97E-05	0,0285	GBP2
237032_x_at	4,89	5,93	-2,05	3,16E-05	0,024	SIPA1L1
227948_at	4,67	5,71	-2,06	3,64E-06	0,0066	FGD4
229584_at	4,79	5,87	-2,11	8,64E-05	0,0435	LRRK2
214841_at	4,44	5,52	-2,12	0,0013	0,1864	CNIH3
227052_at	5,45	6,57	-2,16	5,72E-06	0,0087	SMIM14
211959_at	6,51	7,63	-2,18	0,0013	0,1864	IGFBP5
224894_at	4,59	5,82	-2,35	0,0002	0,0728	YAP1
210772_at	4,73	6,09	-2,55	6,10E-05	0,0349	FPR2
226834_at	4,42	5,79	-2,59	0,0028	0,2613	CLMP
201109_s_at	3,86	5,24	-2,6	0,0171	0,5461	THBS1
205119_s_at	7,17	8,79	-3,06	0,0002	0,0654	FPR1
227662_at	4,61	6,24	-3,09	0,0008	0,1449	SYNPO2
210664_s_at	5,15	6,97	-3,51	9,55E-07	0,0031	TFPI
201110_s_at	3,88	5,71	-3,54	0,0076	0,4158	THBS1
213258_at	5,06	6,99	-3,83	1,16E-06	0,0033	TFPI
205239_at	5,33	7,88	-5,88	0,002	0,227	AREG

Table S6. Most regulated genes in THP1 after 24h

ID	Glycodelin Avg (log2)	no Glycodelin Avg (log2)	Fold Change	P-val	FDR P-val	Gene Symbol
211122_s_at	10,66	7,56	8,6	1,32E-06	0,0021	CXCL11
210163_at	8,15	5,25	7,47	1,75E-06	0,0027	CXCL11
231702_at	7,39	4,51	7,39	4,77E-07	0,0017	TDO2

204103_at	9,02	6,3	6,58	0,0002	0,086	CCL4
216598_s_at	10,57	7,86	6,55	2,76E-08	0,0002	CCL2
205943_at	11,46	8,78	6,38	2,95E-07	0,0011	TDO2
219424_at	7,54	4,91	6,17	8,08E-07	0,0019	EBI3
205114_s_at	10,03	7,67	5,13	0,0008	0,2019	CCL3; CCL3L1; CCL3L3
204475_at	7,58	5,37	4,62	8,90E-11	4,86E-06	MMP1
204533_at	12,94	10,74	4,59	8,21E-07	0,0019	CXCL10
203131_at	8,92	6,76	4,46	5,42E-07	0,0017	PDGFRA
214038_at	11,52	9,43	4,27	6,36E-06	0,0074	CCL8
206134_at	8,13	6,12	4,04	1,04E-06	0,0019	ADAMDEC1
230966_at	8,66	6,68	3,93	6,62E-05	0,0397	IL4I1
215223_s_at	10,49	8,51	3,93	1,73E-08	0,0002	LOC100129518; SOD2
206026_s_at	5,7	3,76	3,83	2,39E-05	0,0182	TNFAIP6
207113_s_at	8,37	6,44	3,81	0,0046	0,5024	TNF
203936_s_at	9,86	7,96	3,74	5,78E-08	0,0004	MMP9
202638_s_at	7,75	5,88	3,66	8,70E-07	0,0019	ICAM1
202859_x_at	8,42	6,59	3,55	0,003	0,4061	CXCL8
212143_s_at	10,46	8,68	3,45	8,70E-05	0,0485	IGFBP3
221477_s_at	9,61	7,83	3,42	5,27E-06	0,0063	LOC100129518; SOD2
220146_at	6,71	4,97	3,33	7,29E-07	0,0019	TLR7
229560_at	6,94	5,25	3,21	3,09E-08	0,0002	TLR8
1566342_at	9,96	8,28	3,19	2,76E-05	0,0204	SOD2
218810_at	8,79	7,14	3,14	5,37E-07	0,0017	ZC3H12A
232504_at	5,47	3,82	3,14	9,34E-07	0,0019	LOC285628
203868_s_at	5,24	3,59	3,13	8,43E-08	0,0005	VCAM1
229435_at	5,68	4,06	3,07	0,0001	0,0618	GLIS3
205242_at	10,13	8,53	3,04	4,74E-06	0,0058	CXCL13
216841_s_at	9,5	7,9	3,03	2,57E-07	0,0011	LOC100129518; SOD2
205959_at	6,21	4,65	2,95	2,70E-07	0,0011	MMP13
210095_s_at	11,53	9,98	2,93	8,93E-05	0,0488	IGFBP3
230258_at	5,85	4,32	2,87	0,0004	0,1254	GLIS3
229947_at	5,76	4,25	2,84	2,25E-06	0,0031	PI15
205463_s_at	8,38	6,87	2,84	3,24E-09	6,85E-05	PDGFA
229830_at	8,13	6,65	2,78	3,76E-09	6,85E-05	
202637_s_at	7,8	6,33	2,76	5,66E-07	0,0017	ICAM1
211506_s_at	7,07	5,62	2,72	0,0002	0,089	CXCL8
216834_at	9,39	7,95	2,72	0,0101	0,6765	RGS1
212190_at	10,77	9,34	2,7	1,09E-07	0,0006	SERPINE2
206157_at	7,03	5,6	2,68	0,0003	0,1083	PTX3
211597_s_at	8	6,59	2,67	1,15E-06	0,002	HOPX
210873_x_at	5,99	4,58	2,66	0,0001	0,0618	APOBEC3A; APOBEC3A_B
227834_at	5,19	3,78	2,65	0,0002	0,0892	TXLNB
202643_s_at	9,11	7,7	2,65	8,98E-07	0,0019	TNFAIP3
208607_s_at	6,93	5,52	2,65	2,99E-06	0,004	SAA1; SAA2; SAA2-SAA4
230233_at	4,19	2,8	2,63	0,0002	0,0735	
204961_s_at	10,32	8,95	2,58	1,83E-05	0,0151	NCF1; NCF1B; NCF1C

220091_at	8,44	7,08	2,56	1,87E-06	0,0028	SLC2A6
227487_s_at	5,49	4,16	2,52	0,001	0,2306	SERPINE2
202988_s_at	7,48	6,15	2,51	0,0104	0,6818	RGS1
210839_s_at	6,88	5,55	2,51	1,56E-05	0,0137	ENPP2
201631_s_at	7,62	6,29	2,51	1,00E-06	0,0019	IER3
203828_s_at	6,1	4,77	2,5	1,66E-06	0,0026	IL32
231577_s_at	8,49	7,16	2,5	0,0006	0,1609	GBP1
209670_at	6,09	4,77	2,5	2,12E-06	0,0031	TRAC
1555756_a_at	6,21	4,89	2,49	0,0002	0,0737	CLEC7A
205681_at	7,13	5,82	2,49	0,0006	0,1706	BCL2A1
203915_at	6,35	5,05	2,48	1,49E-05	0,0136	CXCL9
206025_s_at	5,72	4,43	2,45	2,82E-05	0,0205	TNFAIP6
238727_at	5,9	4,61	2,45	0,0007	0,1836	
211719_x_at	8,38	7,11	2,42	0,0073	0,6075	FN1
202270_at	7,42	6,15	2,41	0,0003	0,0943	GBP1
204470_at	6,59	5,33	2,4	0,0004	0,1262	CXCL1
209774_x_at	5,61	4,35	2,4	0,0015	0,2883	CXCL2
223217_s_at	6,8	5,54	2,39	7,48E-07	0,0019	NFKBIZ
214084_x_at	10,38	9,12	2,38	1,16E-05	0,0116	NCF1
221345_at	5,97	4,74	2,36	0,0014	0,2773	FFAR2
209684_at	8,89	7,67	2,34	0,0009	0,2141	RIN2
216867_s_at	8,59	7,37	2,32	2,48E-06	0,0034	PDGFA
207536_s_at	6,11	4,89	2,32	1,37E-08	0,0002	TNFRSF9
201739_at	10,16	8,95	2,31	0,0042	0,4932	SGK1
202269_x_at	8,58	7,39	2,28	0,0006	0,1609	GBP1
209392_at	7,64	6,46	2,27	0,0001	0,0681	ENPP2
231779_at	7,61	6,44	2,25	0,0016	0,2883	IRAK2
223218_s_at	8,51	7,34	2,25	1,20E-05	0,0117	NFKBIZ
205226_at	6,88	5,72	2,24	1,99E-05	0,016	PDGFRL
210004_at	4,65	3,49	2,24	1,04E-06	0,0019	OLR1
1553141_at	7,14	5,99	2,23	2,40E-05	0,0182	LACC1
1552658_a_at	6,24	5,09	2,23	1,00E-05	0,0102	NAV3
229327_s_at	5,89	4,75	2,21	0,0011	0,2366	
217546_at	4,76	3,62	2,2	0,0003	0,0901	MT1M
202644_s_at	10,27	9,14	2,18	7,47E-06	0,0085	TNFAIP3
210258_at	5,28	4,16	2,17	0,0039	0,4706	RGS13
205476_at	10,21	9,09	2,16	0,0014	0,2765	CCL20
205067_at	8,6	7,48	2,16	9,87E-06	0,0102	IL1B
215078_at	4,53	3,42	2,16	0,0062	0,5715	LOC100129518; SOD2
219386_s_at	9,4	8,29	2,16	0,0006	0,1718	SLAMF8
210495_x_at	8,65	7,54	2,16	0,0046	0,5051	FN1
226237_at	3,78	2,67	2,16	4,05E-06	0,0051	COL8A1
215990_s_at	8,18	7,08	2,15	0,0024	0,3448	BCL6
216442_x_at	8,69	7,6	2,14	0,0063	0,5722	FN1
227458_at	5,92	4,83	2,13	0,0007	0,1792	CD274
202833_s_at	8,76	7,68	2,11	9,12E-06	0,0101	SERPINA1

203477_at	9,07	8	2,11	2,52E-05	0,0189	COL15A1
209031_at	7	5,93	2,1	9,73E-07	0,0019	CADM1
212464_s_at	8,53	7,46	2,1	0,0059	0,5545	FN1
208025_s_at	5,59	4,54	2,08	0,0103	0,6818	HMGA2
202672_s_at	7,94	6,91	2,04	0,0023	0,3419	ATF3
236471_at	5,29	4,26	2,04	0,0002	0,0727	NFE2L3
231513_at	7,87	6,85	2,04	7,93E-07	0,0019	
1555759_a_at	10,38	9,36	2,03	0,0002	0,0694	CCL5
206513_at	7,56	6,55	2,03	0,0004	0,1347	AIM2
39402_at	8,51	7,49	2,02	5,52E-05	0,0355	IL1B
220832_at	5,09	4,09	2	2,85E-05	0,0205	TLR8
209699_x_at	7,55	8,6	-2,06	0,0205	0,8096	AKR1C2

Table S7. Most regulated genes in KHYG-1 after 24h

ID	Glycodelin Avg (log2)	no Glycodelin Avg (log2)	Fold Change	P-val	FDR P-val	Gene Symbol
202330_s_at	6,17	4,36	3,52	0,0382	0,3908	UNG
205034_at	5,73	3,93	3,49	0,0178	0,3905	CCNE2
211814_s_at	5,31	3,57	3,33	0,0405	0,3923	CCNE2
229450_at	4,97	3,25	3,3	0,0017	0,3905	IFIT3
210354_at	5,1	3,44	3,17	0,0002	0,3905	IFNG
204103_at	11,04	9,38	3,16	0,0003	0,3905	CCL4
216248_s_at	4,36	2,78	2,99	4,09E-05	0,3905	NR4A2
203967_at	6,61	5,1	2,85	0,034	0,3908	CDC6
220651_s_at	4,89	3,4	2,81	0,0054	0,3905	MCM10
203126_at	5,55	4,06	2,8	0,0158	0,3905	IMPA2
225655_at	7,63	6,16	2,77	0,0237	0,3905	UHRF1
204622_x_at	4,92	3,45	2,76	5,40E-05	0,3905	NR4A2
206365_at	7,15	5,69	2,76	0,0001	0,3905	XCL1
207535_s_at	5,67	4,24	2,68	0,0114	0,3905	NFKB2
1557129_a_at	3,99	2,61	2,6	0,0013	0,3905	FAM111B
219288_at	5,57	4,21	2,56	0,0028	0,3905	C3orf14
228033_at	5,17	3,84	2,5	0,0134	0,3905	E2F7
221521_s_at	7,33	6,03	2,46	0,033	0,3908	GINS2
219990_at	6,41	5,15	2,39	0,0112	0,3905	E2F8
209891_at	6,91	5,67	2,37	0,0014	0,3905	SPC25
1552470_a_at	4,57	3,34	2,35	0,0191	0,3905	ABHD11
210567_s_at	5,47	4,24	2,34	0,0034	0,3905	SKP2
231164_at	6,72	5,5	2,33	0,0038	0,3905	ABCA17P
211162_x_at	6,73	5,53	2,3	0,0003	0,3905	SCD
222680_s_at	7,26	6,09	2,26	0,0308	0,3908	DTL
207113_s_at	6,63	5,46	2,25	0,0003	0,3905	TNF
204621_s_at	3,91	2,74	2,25	0,0032	0,3905	NR4A2
207339_s_at	9,08	7,92	2,23	0,0162	0,3905	LTB
203210_s_at	6,54	5,41	2,18	0,0103	0,3905	RFC5

223307_at	8,34	7,22	2,18	0,0001	0,3905	CDCA3
202068_s_at	7,58	6,46	2,17	0,0041	0,3905	LDLR
242918_at	5,35	4,24	2,16	0,0029	0,3905	NASP
242069_at	5,79	4,68	2,16	0,0019	0,3905	CBX5
212791_at	5,79	4,68	2,16	0,019	0,3905	C1orf216
216228_s_at	4,59	3,48	2,16	0,0054	0,3905	WDHD1

Table S8: Cox-regression of immunotherapy cohort

CI = confidencial interval, ECOG = Eastern Cooperative Oncology Group

Parameter	Hazard Ratio (95% CI)	p-value
Glycodelin high	1.458 (0.899-2.365)	0.127
Progesterone high	1.694 (1.066-2.692)	**0.026**
Immunotherapie line	1.149 (0.876-1.506)	0.316
Sex (f vs male)	1.347 (0.849-2.136)	0.206
Age at diagnosis	1.016 (0.989-1.043)	0.251
ECOG	1.068 (0.683-1.671)	0.771
Stage at diagnosis	0.871 (0.659-1.151)	0.331

Declarations

Ethics approval and consent to participate

All procedures were conducted in accordance with the Ethics committee Heidelberg and study protocol was proofed (S-827/2020).

Consent for publication

Available on request (Broad Consent of Lung Biobank Heidelberg, Ethics approval S-270/2001)

Availability of data and materials

Affymetrix gene expression data have been deposited in NCBI's Gene Expression Omnibus and are accessible through GEO Series accession number GSE222124. Original immunoblot images are accessible on request.

Competing interests

The authors declare that they have no competing interests.

Funding

This work was supported by the German Ministry of Education and Research (BMBF), as part of the German Center for Lung Research (82DZL00402, 82DZL001A5, 82DZL00404). HK acknowledges support from Sigrid Jusélius Foundation.

Authors' contributions

Conceptualization – MAS, SR, TM, MM, UK

Methodology – SR, MAS, SM, HW, PC, HK

Formal Analysis – MAS

Software – SR, SM, TM, MAS

Investigation – SR, MAS, SM, MA

Writing – SR, MAS

Review and editing – all authors

Funding Acquisition – MT, UK, SM, MAS, MM, HK

Supervision – MAS, UK

Acknowledgements

We would like to thank Christa Stolp, Andrea Kreß, Carmen Hoppstock, Martin Fallenbuechel, Elizabeth Xu Meister, and Annikki Ljöfhelm for expert technical support. We would like to thank the NCT tissue bank and Christiane Zorzgelski for providing the TMAs. Moreover, we thank Felix Gruenewald from ROCHE for provision of the glycodelin antibody.

References

1. Globocan, IARC. (https://gco.iarc.fr/today/home, 2020).
2. F. Bray *et al.*, Global cancer statistics 2018: GLOBOCAN estimates of incidence and mortality worldwide for 36 cancers in 185 countries. *CA Cancer J Clin* **68**, 394-424 (2018).
3. M. Reck *et al.*, Updated Analysis of KEYNOTE-024: Pembrolizumab Versus Platinum-Based Chemotherapy for Advanced Non-Small-Cell Lung Cancer With PD-L1 Tumor Proportion Score of 50% or Greater. *J Clin Oncol* **37**, 537-546 (2019).
4. Z. Y. Xu-Monette, M. Zhang, J. Li, K. H. Young, PD-1/PD-L1 Blockade: Have We Found the Key to Unleash the Antitumor Immune Response? *Front Immunol* **8**, 1597 (2017).
5. J. M. Taube *et al.*, Colocalization of inflammatory response with B7-h1 expression in human melanocytic lesions supports an adaptive resistance mechanism of immune escape. *Sci Transl Med* **4**, 127ra137 (2012).
6. M. Seppala, H. Bohn, Y. Tatarinov, Glycodelins. *Tumour Biol* **19**, 213-220 (1998).
7. L. Sawyer, beta-Lactoglobulin and Glycodelin: Two Sides of the Same Coin? *Front Physiol* **12**, 678080 (2021).
8. J. Garde, S. C. Bell, I. C. Eperon, Multiple forms of mRNA encoding human pregnancy-associated endometrial alpha 2-globulin, a beta-lactoglobulin homologue. *Proc Natl Acad Sci U S A* **88**, 2456-2460 (1991).
9. N. A. Bersinger, M. H. Birkhauser, M. Yared, D. M. Wunder, Serum glycodelin pattern during the menstrual cycle in healthy young women. *Acta Obstet Gynecol Scand* **88**, 1215-1221 (2009).
10. M. Seppala, R. N. Taylor, H. Koistinen, R. Koistinen, E. Milgrom, Glycodelin: a major lipocalin protein of the reproductive axis with diverse actions in cell recognition and differentiation. *Endocr Rev* **23**, 401-430 (2002).
11. A. Schiefner, F. Rodewald, I. Neumaier, A. Skerra, The dimeric crystal structure of the human fertility lipocalin glycodelin reveals a protein scaffold for the presentation of complex glycans. *Biochem J* **466**, 95-104 (2015).
12. W. S. Yeung *et al.*, Effects of glycodelins on functional competence of spermatozoa. *J Reprod Immunol* **83**, 26-30 (2009).
13. H. R. Morris *et al.*, Gender-specific glycosylation of human glycodelin affects its contraceptive activity. *J Biol Chem* **271**, 32159-32167 (1996).
14. H. Koistinen *et al.*, Differences in glycosylation and sperm-egg binding inhibition of pregnancy-related glycodelin. *Biol Reprod* **69**, 1545-1551 (2003).

796 15. C. L. Lee *et al.*, The Pleiotropic Effect of Glycodelin-A in Early Pregnancy. *Am J Reprod Immunol*
797 **75**, 290-297 (2016).
798 16. S. G. Holtan, D. J. Creedon, P. Haluska, S. N. Markovic, Cancer and pregnancy: parallels in
799 growth, invasion, and immune modulation and implications for cancer therapeutic agents.
800 *Mayo Clin Proc* **84**, 985-1000 (2009).
801 17. H. Koistinen *et al.*, The role of glycodelin in cell differentiation and tumor growth. *Scand J Clin*
802 *Lab Invest* **69**, 452-459 (2009).
803 18. S. Ren *et al.*, Functional characterization of the progestagen-associated endometrial protein
804 gene in human melanoma. *J Cell Mol Med* **14**, 1432-1442 (2010).
805 19. M. A. Schneider *et al.*, Glycodelin: A New Biomarker with Immunomodulatory Functions in
806 Non-Small Cell Lung Cancer. *Clin Cancer Res* **21**, 3529-3540 (2015).
807 20. M. A. Schneider *et al.*, Glycodelin as a Serum and Tissue Biomarker for Metastatic and
808 Advanced NSCLC. *Cancers (Basel)* **10**, (2018).
809 21. C. Soni, A. A. Karande, Glycodelin A suppresses the cytolytic activity of CD8+ T lymphocytes.
810 *Mol Immunol* **47**, 2458-2466 (2010).
811 22. S. Gottschling *et al.*, Establishment and comparative characterization of novel squamous cell
812 non-small cell lung cancer cell lines and their corresponding tumor tissue. *Lung Cancer* **75**, 45-
813 57 (2012).
814 23. S. A. Bustin *et al.*, The MIQE guidelines: minimum information for publication of quantitative
815 real-time PCR experiments. *Clin Chem* **55**, 611-622 (2009).
816 24. W. D. Travis, E. Brambilla, A. P. Burke, A. Marx, A. G. Nicholson, Introduction to The 2015 World
817 Health Organization Classification of Tumors of the Lung, Pleura, Thymus, and Heart. *J Thorac*
818 *Oncol* **10**, 1240-1242 (2015).
819 25. S. Mirsadraee, D. Oswal, Y. Alizadeh, A. Caulo, E. van Beek, Jr., The 7th lung cancer TNM
820 classification and staging system: Review of the changes and implications. *World J Radiol* **4**,
821 128-134 (2012).
822 26. H. Koistinen *et al.*, Glycodelin from seminal plasma is a differentially glycosylated form of
823 contraceptive glycodelin-A. *Mol Hum Reprod* **2**, 759-765 (1996).
824 27. J. Budczies *et al.*, Cutoff Finder: a comprehensive and straightforward Web application
825 enabling rapid biomarker cutoff optimization. *PLoS One* **7**, e51862 (2012).
826 28. C. L. Lee *et al.*, Glycodelin-A as a paracrine regulator in early pregnancy. *J Reprod Immunol* **90**,
827 29-34 (2011).
828 29. H. Uchida *et al.*, Glycodelin in reproduction. *Reprod Med Biol* **12**, 79-84 (2013).
829 30. A. Alok, D. Mukhopadhyay, A. A. Karande, Glycodelin A, an immunomodulatory protein in the
830 endometrium, inhibits proliferation and induces apoptosis in monocytic cells. *Int J Biochem*
831 *Cell Biol* **41**, 1138-1147 (2009).
832 31. J. Rachmilewitz, G. J. Riely, M. L. Tykocinski, Placental protein 14 functions as a direct T-cell
833 inhibitor. *Cell Immunol* **191**, 26-33 (1999).
834 32. A. E. Bolton *et al.*, Identification of placental protein 14 as an immunosuppressive factor in
835 human reproduction. *Lancet* **1**, 593-595 (1987).
836 33. M. Julkunen *et al.*, Distribution of placental protein 14 in tissues and body fluids during
837 pregnancy. *Br J Obstet Gynaecol* **92**, 1145-1151 (1985).
838 34. M. Seppala, H. Koistinen, R. Koistinen, P. C. Chiu, W. S. Yeung, Glycosylation related actions of
839 glycodelin: gamete, cumulus cell, immune cell and clinical associations. *Hum Reprod Update*
840 **13**, 275-287 (2007).
841 35. M. Seppala *et al.*, Glycodelin in reproductive endocrinology and hormone-related cancer. *Eur*
842 *J Endocrinol* **160**, 121-133 (2009).
843 36. T. Okazaki, T. Honjo, PD-1 and PD-1 ligands: from discovery to clinical application. *Int Immunol*
844 **19**, 813-824 (2007).
845 37. H. Borghaei *et al.*, Nivolumab versus Docetaxel in Advanced Nonsquamous Non-Small-Cell
846 Lung Cancer. *N Engl J Med* **373**, 1627-1639 (2015).
847 38. J. R. Brahmer *et al.*, Safety and activity of anti-PD-L1 antibody in patients with advanced cancer.
848 *N Engl J Med* **366**, 2455-2465 (2012).

39. M. Seppala, H. Koistinen, R. Koistinen, Glycodelins. *Trends Endocrinol Metab* **12**, 111-117 (2001).
40. D. Mukhopadhyay, S. Sundereshan, C. Rao, A. A. Karande, Placental protein 14 induces apoptosis in T cells but not in monocytes. *J Biol Chem* **276**, 28268-28273 (2001).
41. G. Mishan-Eisenberg *et al.*, Differential regulation of Th1/Th2 cytokine responses by placental protein 14. *J Immunol* **173**, 5524-5530 (2004).
42. S. SundarRaj, C. Soni, A. A. Karande, Glycodelin A triggers T cell apoptosis through a novel calcium-independent galactose-binding lectin activity. *Mol Immunol* **46**, 3411-3419 (2009).
43. K. K. Lam *et al.*, Glycodelin-A protein interacts with Siglec-6 protein to suppress trophoblast invasiveness by down-regulating extracellular signal-regulated kinase (ERK)/c-Jun signaling pathway. *J Biol Chem* **286**, 37118-37127 (2011).
44. C. L. Lee *et al.*, Glycodelin-A stimulates the conversion of human peripheral blood CD16-CD56bright NK cell to a decidual NK cell-like phenotype. *Hum Reprod* **34**, 689-701 (2019).
45. E. Ish-Shalom *et al.*, alpha2,6-Sialylation promotes binding of placental protein 14 via its Ca2+-dependent lectin activity: insights into differential effects on CD45RO and CD45RA T cells. *Glycobiology* **16**, 173-183 (2006).
46. A. Montfort *et al.*, The TNF Paradox in Cancer Progression and Immunotherapy. *Front Immunol* **10**, 1818 (2019).
47. B. K. Lo *et al.*, CXCR3/ligands are significantly involved in the tumorigenesis of basal cell carcinomas. *Am J Pathol* **176**, 2435-2446 (2010).
48. H. Okada, Brain tumor immunotherapy with type-1 polarizing strategies. *Ann N Y Acad Sci* **1174**, 18-23 (2009).
49. J. Gong, A. Chehrazi-Raffle, S. Reddi, R. Salgia, Development of PD-1 and PD-L1 inhibitors as a form of cancer immunotherapy: a comprehensive review of registration trials and future considerations. *J Immunother Cancer* **6**, 8 (2018).
50. R. A. M. Wilson, T. R. J. Evans, A. R. Fraser, R. J. B. Nibbs, Immune checkpoint inhibitors: new strategies to checkmate cancer. *Clin Exp Immunol* **191**, 133-148 (2018).
51. P. Sinha, V. K. Clements, S. Ostrand-Rosenberg, Reduction of myeloid-derived suppressor cells and induction of M1 macrophages facilitate the rejection of established metastatic disease. *J Immunol* **174**, 636-645 (2005).
52. J. Yan, X. Wu, J. Yu, Y. Zhu, S. Cang, Prognostic Role of Tumor Mutation Burden Combined With Immune Infiltrates in Skin Cutaneous Melanoma Based on Multi-Omics Analysis. *Front Oncol* **10**, 570654 (2020).
53. P. M. Ellis, E. T. Vella, Y. C. Ung, Immune Checkpoint Inhibitors for Patients With Advanced Non-Small-Cell Lung Cancer: A Systematic Review. *Clin Lung Cancer* **18**, 444-459 e441 (2017).
54. G. L. Beatty, W. L. Gladney, Immune escape mechanisms as a guide for cancer immunotherapy. *Clin Cancer Res* **21**, 687-692 (2015).
55. J. Xiao, L. Zhou, B. He, Q. Chen, Impact of Sex and Smoking on the Efficacy of EGFR-TKIs in Terms of Overall Survival in Non-small-Cell Lung Cancer: A Meta-Analysis. *Front Oncol* **10**, 1531 (2020).
56. A. Grassadonia *et al.*, Effect of Gender on the Outcome of Patients Receiving Immune Checkpoint Inhibitors for Advanced Cancer: A Systematic Review and Meta-Analysis of Phase III Randomized Clinical Trials. *J Clin Med* **7**, (2018).
57. S. Madala *et al.*, Gender Differences and Their Effects on Survival Outcomes in Lung Cancer Patients Treated With PD-1/PD-L1 Checkpoint Inhibitors: A Systematic Review and Meta-Analysis. *Clin Oncol (R Coll Radiol)* **34**, 799-809 (2022).
58. G. Kichenadasse *et al.*, Association Between Body Mass Index and Overall Survival With Immune Checkpoint Inhibitor Therapy for Advanced Non-Small Cell Lung Cancer. *JAMA Oncol* **6**, 512-518 (2020).
59. T. B. Trefzer *et al.*, Intratumoral Heterogeneity and Immune Modulation in Lung Adenocarcinoma in Female Smokers and Never Smokers. *Cancer Res* **82**, 3116-3129 (2022).
60. F. Conforti *et al.*, Cancer immunotherapy efficacy and patients' sex: a systematic review and meta-analysis. *Lancet Oncol* **19**, 737-746 (2018).

902 61. C. J. D. Wallis *et al.*, Association of Patient Sex With Efficacy of Immune Checkpoint Inhibitors
903 and Overall Survival in Advanced Cancers: A Systematic Review and Meta-analysis. *JAMA Oncol*
904 **5**, 529-536 (2019).
905 62. D. C. Marquez-Garban *et al.*, Progesterone and estrogen receptor expression and activity in
906 human non-small cell lung cancer. *Steroids* **76**, 910-920 (2011).
907 63. C. L. Clarke, R. L. Sutherland, Progestin regulation of cellular proliferation. *Endocr Rev* **11**, 266-
908 301 (1990).

909